

OPTIMAL SEQUENCING DEPTH FOR SINGLE-CELL RNA-SEQUENCING IN WASSERSTEIN SPACE

BY JAKWANG KIM^{1,a*}, SHARVAJ KUBAL^{2,b} AND GEOFFREY SCHIEBINGER^{2,c}

¹*School of Data Science, The Chinese University of Hongkong, Shenzhen, Guangdong, China*, ^ajakwangkim@cuhk.edu.cn

²*Department of Mathematics, University of British Columbia, Vancouver, British Columbia, Canada*, ^bsharvaj@math.ubc.ca;
^cgeoff@math.ubc.ca

How many samples should one collect for an empirical distribution to be as close as possible to the true population? This question is not trivial in the context of single-cell RNA-sequencing. With limited sequencing depth, profiling more cells comes at the cost of fewer reads per cell. Therefore, one must strike a balance between the number of cells sampled and the accuracy of each measured gene expression profile. In this paper, we analyze an empirical distribution of cells and obtain upper and lower bounds on the Wasserstein distance to the true population. Our analysis holds for general, non-parametric distributions of cells, and is validated by simulation experiments on a real single-cell dataset.

1. Introduction. The recent success of single-cell RNA sequencing (scRNA-seq) technologies [40, 45] has resulted in massive, high-dimensional datasets, which invite interesting statistical questions. There has been intensive work on clustering of cells [26, 71], transformations and variance stabilization [1], trajectory inference [42, 61, 65] and manifold learning and denoising [32, 74]. Mathematically, the basic input in each of these tasks is an empirical distribution of cells; these are the cells sampled by scRNA-seq. However, contrary to the ordinary setting of high-dimensional statistics, the support of the empirical distribution is also noisy. This is because cells' gene expression profiles are measured, through sequencing, with finitely many 'reads'.

A 'read' is the fundamental unit of information in DNA sequencing, and in RNA sequencing for that matter. The relative abundances of gene transcripts, which characterize cell type, can be measured by extracting RNA from the cell, and reading the sequence of nucleotide letters (ACTG) using a DNA sequencing machine. Each 'read' documents the presence of one molecule of RNA in one cell. Early forms of single-cell RNA sequencing produced high-fidelity measurements of gene expression by profiling small numbers of cells, with a large number of reads per cell. Droplet-based technologies made it possible to profile vastly more cells, but with fewer reads per cell. It soon became clear that this was beneficial for identifying rare cell types in complex populations of cells [2, 15, 19, 29, 34, 58, 67, 69].

The natural experimental design question is the following: given a finite budget of reads, how many cells should be profiled so that the empirical distribution is as close as possible to the true population? As illustrated in Figure 1, profiling fewer cells allows each expression profile to be measured more accurately (with more reads per cell), but the full population is not well explored. On the other hand, profiling more cells gives an empirical distribution with larger support, but with more noise in the support which can blur out the finer features of the population distribution such as the two clusters (the peaks in the shaded contour plots).

*This work was done when this author was at department of mathematics of University of British Columbia.
MSC2020 subject classifications: Primary 62G05, 49Q22; secondary 62D99.

Keywords and phrases: RNA sequencing, optimal transport, Wasserstein distance, optimal depth, empirical distribution, nonparametric inference.

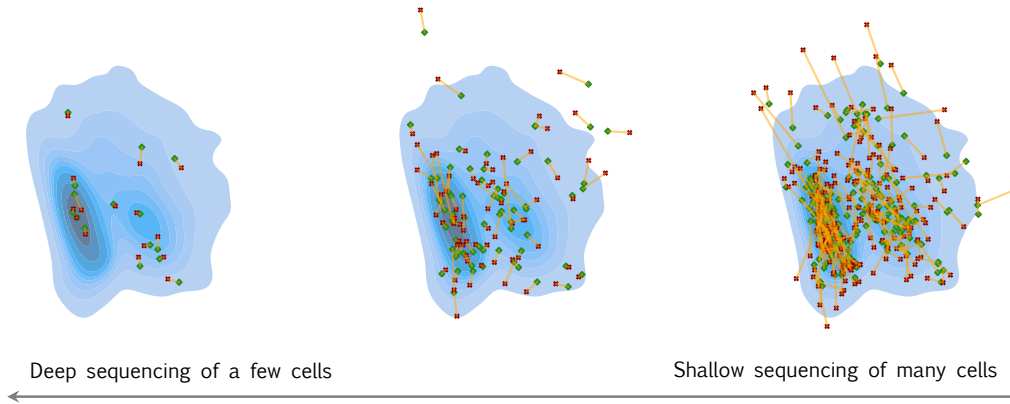


FIGURE 1. **The trade-off between deep and shallow sequencing.** In this schematic, we have three panels illustrating the effect of different sequencing depths. In each panel, the shaded contours describe the unknown distribution of gene expression in a population of cells. The green dots represent the true gene expressions of sampled cells, whereas the red markers indicate the corresponding measured gene expressions obtained via the sequencing process. The yellow lines match a cell’s true and measured gene expressions. When the number of cells is very low (left panel), each cell receives a high proportion of the budget of reads, leading to low measurement noise. However, the population distribution is not well-captured. Conversely, when the number of cells is very high (right panel), each cell receives a small fraction of the budget, resulting in very noisy measurements. The central panel depicts an intermediate case that balances these two effects.

Due to its importance, there have been a lot of works [30, 34, 58, 67, 69, 78, 82] which try to answer this question with a certain assumption. In this work, we analyze this experimental design question in a very general setting. We leverage *optimal transport*, more precisely *Wasserstein distance*, to evaluate the discrepancy between the noisy empirical distribution obtained by RNA sequencing and the unknown ground truth. There are many advantages of using optimal transport. First, it is well defined for the comparison between sufficiently general probability distributions. Moreover, Wasserstein distance takes into account *not vertical but horizontal difference between distributions*, which displays geometric information of distributions. Most classical divergences, for example, Kullback–Leibler divergence, or the total variation distance are useless to understand the rate of convergence of empirical distributions. Wasserstein distance, on the other hand, is useful for it since it measures the cost of transporting mass from one to other place, hence the difference of distributions horizontally. We refer the readers to [64][Figure 5.1]. Second, Wasserstein geometry naturally involves *gradient flow*, the evolution of distributions [4, 48, 49, 55]. Since the recent demands of trajectory inference in single-cell RNA-sequencing data have emerged [42, 61, 65], Wasserstein geometry and Wasserstein gradient flows are the state-of-art mathematical tool for this field. Lastly, Wasserstein distance is *computationally tractable*. In his seminar work, Cuturi [14] proposed an almost linear-complexity approximation algorithm, the so-called Sinkhorn algorithm or entropic optimal transport, which allows practitioners to use it in reality.

In this flexible framework, we are able to obtain results for general distributions of cells, without any assumptions on the distribution of interest. Moreover, because we focus on the empirical distribution directly, and not on any specific estimator, we hope that our results can inform broad estimation tasks. Our result depends on the sparsity of gene expression and the intrinsic low dimensionality of its distribution explicitly, which explains the role of those factors in RNA sequencing in a clear way. Furthermore, we conduct simulation experiments on a real single-cell dataset to validate and support the theory.

1.1. *Setup and contributions.* In this section, we introduce the mathematical notation and the setting of the problem, and state our contribution. Throughout this paper, d , n and m denote the number of genes, i.e. the dimension of gene expression vector, the number of cells, and the number of reads, respectively. In the sequel we use big- O notation as usual, $f(n) \sim g(n)$ if f and g have the same first order growth, and $f(n) \lesssim g(n)$ if $f(n)$ is less than $g(n)$ in terms of variables of interest while other universal constants are fixed.

We model the measurement process with two steps. The first step is the selection of n cells from the population. This will give us an empirical distribution of cells μ_n , defined precisely in (1.1) below. Then, in the second step, we measure the gene expression of each cell through sequencing to obtain a noisy empirical distribution $\hat{\mu}_n(m)$, defined precisely in (1.2) below.

In sequencing, only the relative abundance of gene products matters. Therefore, we represent gene expression profiles of cells in relative terms. We denote a cell's gene expression vector by $X = (x_1, \dots, x_d) \in \Delta_{(d-1)}$ where $\Delta_{(d-1)}$ is the $(d-1)$ -dimensional simplex. A population of cells is represented by a probability measure μ on Δ_{d-1} , i.e., X is distributed according to μ . In practice, despite the large d , the distribution μ enjoys nice low dimensional structure, quantified here by an *intrinsic dimension* k which will be defined rigorously later (see Theorem 2.1 and Theorem 2.2). Our goal is to obtain a distribution which approximates μ .

In the first step of the measurement process, we sample n cells from the population. This gives us i.i.d. samples from μ which we denote by $\mathbf{X} := \{X_1, \dots, X_n\} \subseteq \Delta_{(d-1)}$. We denote the unknown true empirical distribution by

$$(1.1) \quad \mu_n := \frac{1}{n} \sum_{i=1}^n \delta_{X_i}.$$

In the second step of the measurement process, we consider two related models for the sequencing procedure. In both cases, cell expression profiles are generated multinomially from the true expression profile. The two models differ in how many reads are selected per cell. In the first model, cell sampling frequency $U \in \mathbb{R}_{>0}$ can depend on gene expression profile X . In the second model, X and U are independent. Model 1 accounts for the fact that larger cells contain more molecules of RNA, whereas model 2 accounts for the cell-type independent factors such as RNA capture efficiency. We use $\mu_{(X,U)}$ to denote the joint distribution of U and X for the first model. When we write μ with no subscript, it denotes the (marginal) distribution of X .

Given cells $X_1, \dots, X_n \in \Delta_{d-1}$ with sampling frequencies $U_1, \dots, U_n \in \mathbb{R}_{>0}$, we sample m i.i.d. reads to obtain noisy expression profiles $\hat{X}_1, \dots, \hat{X}_n \in \Delta_{(d-1)}$ as follows:

$$\hat{X}_i \sim \frac{1}{m_i} \text{Multinomial}(X_i, m_i),$$

where $(m_1, \dots, m_n) \sim \text{Multinomial}(\mathbf{u}, m)$, and $\mathbf{u} = (u_1, \dots, u_n)$ such that u_i 's are normalized sampling frequencies, i.e., $u_i := \frac{U_i}{\sum_j U_j}$, for $i = 1, \dots, n$. For the case that $m_i = 0$, which would happen with small but positive probability, we choose \hat{X}_i arbitrarily from Δ_{d-1} . Finally, the *noisy empirical distribution* is obtained as

$$(1.2) \quad \hat{\mu}_n(m) := \frac{1}{n} \sum_{i=1}^n \delta_{\hat{X}_i}.$$

Note that variants of such a multinomial sequencing model are standard in the literature [30, 70], and are closely related to the popular Poisson model [78, 82].

Then, the goal is to answer two questions on $\hat{\mu}_n(m)$, the output of shallow sequencing, in order to promise the closeness of $\hat{\mu}_n(m)$ to μ :

- (I) given n cells, how many reads at least should we use to obtain good $\hat{\mu}_n(m)$,
- (II) given m reads, how many cells at most can we use to obtain the best $\hat{\mu}_n(m)$.

In Theorem 2.4 and Theorem 2.5, we resolve question (I) by showing that $m \gtrsim \frac{n}{\varepsilon^2}$ is sufficient to guarantee that Wasserstein distance between $\hat{\mu}_n(m)$ and μ_n is less than ε , and the expected Wasserstein distance between $\hat{\mu}_n(m)$ and μ_n is lower bounded by $\frac{n}{m}$ in general. Built from these results, we show that $n \sim m^{1-\frac{2}{\kappa+2}}$ is optimal in Theorem 2.6, Theorem 2.8 and Theorem 2.9, which solves question (II). In particular, our results depend on the sparsity and the intrinsic dimension explicitly, which illustrates their effectiveness to approximation.

1.2. *Comparison to related work.* The power of shallow sequencing was first explored by Jaitin et al. [34] and Shalek et al. [67] as they propelled single-cell sequencing technologies towards high throughput regimes. Their experiments were followed by a comprehensive analysis [58] and a commentary [69], establishing the validity and benefits of shallow sequencing for various downstream tasks. In particular, Pollen et al. [58] demonstrated that shallow sequencing (up to a certain level) is sufficient for cell-type classification and clustering, even when subgroup differences are subtle. Additionally, they tracked the performance of principal component analysis (PCA), showing that PCA eigenvectors and sample scores correlate strongly between deep- and shallow-sequenced versions of the same dataset.

Variants of this experimental design question have been analyzed [30, 82]. Heimberg et al. [30] analyzed the error in *principal components* incurred with shallow sequencing. Masoero et al. [46] have addressed a related but different experimental design question for variant calling in genome sequencing.

The initial work mentioned above was followed up by Heimberg et al. [30], whose key theoretical contribution involves quantifying the difference between the PCA eigenvectors of a "ground truth" gene expression dataset and the corresponding PCA eigenvectors of its shallow-sequenced version. In terms of our framework, these are the eigenvectors of the covariance matrices Σ_n and $\hat{\Sigma}_n(m)$ of the true empirical distribution μ_n and the noisy empirical distribution $\hat{\mu}_n(m)$ respectively. In such a setting, Heimberg et al. [30, Eq. 2] provide a read depth calculator for optimal budget allocation. Let $v_i \in \mathbb{R}^d$ and $\lambda_i \geq 0$ be the i -th eigenvector and eigenvalue of Σ_n respectively, and let $\hat{v}_i \in \mathbb{R}^d$ be the i -th eigenvector of $\hat{\Sigma}_n(m)$. They prescribe the allocation

$$(1.3) \quad \frac{m}{n} \sim \frac{\kappa^2}{n\lambda_i\varepsilon^2}$$

where $\varepsilon > 0$ is the desired error such that $\|v_i - \hat{v}_i\|_2 \leq \varepsilon$, and κ is a constant that can be estimated from existing data. The allocation (1.3) is interesting since the number of cells n cancels out, having no direct effect on the eigenvector error. Nevertheless, (1.3) does not address our problem of estimating the *population* distribution μ or its associated quantities, since v_1, \dots, v_d are the principal directions of the *empirical* distribution μ_n and not of the population μ . In that direction, it may be more meaningful to compare $\hat{\Sigma}_n$ with the population covariance Σ (i.e. covariance of μ).

Estimating population distributions in this context was first addressed by Wang et al. [78] and Zhang, Ntranos and Tse [82], and both relied on empirical Bayes (EB) deconvolution techniques of Efron [20]. Zhang, Ntranos and Tse [82] established minimax rates of $\Theta(\frac{1}{m})$ for various estimation problems including 1-dimensional marginals, moments, and pairwise moments. They also investigated optimal sequencing budget allocation for the number of reads m and cells n , and showed that the minimax rate can be achieved by empirical Bayes estimators as long as

$$(1.4) \quad \frac{m}{nd} = \Theta(1)$$

(see [82, Theorems 1 and 2]). However, their results do not cover estimation of high-dimensional, non-parametric distributions.

We study the optimal allocation problem in a high-dimensional, non-parametric setting for the first time to our knowledge. Our allocation $n \sim \left(\frac{m}{\mathbb{E}\|X\|_0}\right)^{1-\frac{2}{k+2}}$ (see Theorem 2.8) yields the rate

$$\mathbb{E}W_p(\widehat{\mu}_n(m), \mu) \leq O\left(\left(\frac{\mathbb{E}\|X\|_0}{m}\right)^{\frac{1}{2+k}}\right)$$

which explicitly incorporates the intrinsic dimension k and the average sparsity $\mathbb{E}\|X\|_0$. Moreover, we note that the linear allocation (1.4) of Zhang, Ntranos and Tse [82] is similar to our result when k is large, but it is not quite optimal in our setting; it can suffer from a non-diminishing error $\mathbb{E}W_p(\widehat{\mu}_n(m), \mu) = \Theta(1)$ under certain assumptions (see Theorem 2.9).

1.3. Organization. In Section 2, some background of optimal transport, stochastic dominance and multinomial sampling (Section 2.1) and our main results (Section 2.2) will be provided. In Section 3, we will give an empirical evidence based on the real data set of Schiebinger et al. [65]. Proofs of main results will be presented in Section 4. Lastly, we will summarize our contribution and discuss some future directions in Section 5.

2. Main results.

2.1. Preliminaries. In the present paper, Wasserstein distance is the quantity to measure the goodness of the noisy empirical distribution.

Let's discuss the history of optimal transport very briefly. Optimal transport(OT) has a long story and is an interdisciplinary field connecting to both pure mathematics and applied sciences. Proposed by Monge [52], optimal transport was developed by Kantorovich [35, 36] developed a standard framework for analyzing optimal transport, for which he received Nobel prize in economic sciences. Since then, OT has related to PDE, geometry and probability [4, 9–12, 21, 22, 25, 37, 44, 48, 55, 56]. Recently, OT has also played a central role in finance, statistics and machine learning: model free approach in mathematical finance and its statistical inference [3, 31, 38], optimization of mean field two-layer neural networks [13, 50, 63, 68], diffusion model [16, 28, 79], variational inference [17, 41] and adversarial training [59, 72, 73].

Given spaces \mathcal{X} and \mathcal{Y} , and “cost function” $c : \mathcal{X} \times \mathcal{Y} \rightarrow \mathbb{R} \cup \{-\infty, +\infty\}$, the *Monge problem* (named for a special case proposed in [52]) is to find a map $T : \mathcal{X} \rightarrow \mathcal{Y}$ which achieves the minimum of the following optimization problem:

$$\inf_{(T)_\#(\mu)=\nu} \int_{\mathcal{X}} c(x, T(x)) d\mu(x)$$

where $(T)_\#(\mu)$ is a pushforward measure, i.e. $(T)_\#(\mu)(B) := \mu(T^{-1}(B))$ for any measurable function T and measurable subset B . It is well known that, however, such a T may not exist even for nice c . For the well-definedness of the problem, Kantorovich extended the solution space of the Monge problem to the set of couplings of marginals [35, 36]. The problem becomes an infinite dimensional linear optimization problem, which is defined as

$$\min_{\pi \in \Pi(\mu, \nu)} \int_{\mathcal{X} \times \mathcal{Y}} c(x, y) d\pi(x, y).$$

If the spaces \mathcal{X} and \mathcal{Y} are Polish(complete and metrizable), then $\Pi(\mu, \nu)$ is non-empty and compact with respect to weak topology. For nonnegative and lower semi-continuous c , a minimizer of Kantorovich's problem always exists [76, Theorem 4.1].

The Kantorovich formulation provides a rich mathematical framework: it can be leveraged to define a distinguished family of metrics on the space of probability measures. Let $\mathcal{X} = \mathcal{Y}$ be a Polish (complete metric) space. The p -Wasserstein distance, or Kantorovich-Rubinstein distance, is defined over $\mathcal{P}_p(\mathcal{X})$, as follows:

$$W_p(\mu, \nu) := \min_{\pi \in \Pi(\mu, \nu)} \left(\int_{\mathcal{X} \times \mathcal{X}} \text{dist}(x, y)^p d\pi(x, y) \right)^{\frac{1}{p}}.$$

Let $\mathcal{P}_p(\mathcal{X})$ denote the set of probability measures over \mathcal{X} with finite p -th order moment. It is well known that $\mathcal{P}_p(\mathcal{X})$ equipped with W_p is a metric space. In addition, $(\mathcal{P}_2(\mathcal{X}), W_2)$ carries Riemannian structure [55], which generates plentiful implications in many fields in mathematics. Recently, even this space plays numerous roles in many different sciences, especially machine learning and statistics: see Peyré and Cuturi [57].

In the sequel, we will utilize recent progresses concerning the rate of convergence of empirical distributions from Niles-Weed and Bach [53]. To state them rigorously, we need to introduce Wasserstein dimension.

DEFINITION 2.1. [53] Let $(\mathcal{F}, \|\cdot\|)$ be a (semi)normed space. Given a set $S \subseteq \mathcal{F}$, the ε -covering number of S , denoted by $\mathcal{N}(\varepsilon, S, \|\cdot\|)$, is the minimum m such that there exist m closed balls B_1, \dots, B_m of diameter ε such that $S \subseteq \cup_{i=1}^m B_i$. The centers of the balls need not belong to S . The ε -dimension of S is defined as

$$d(\varepsilon; S) := \frac{\log \mathcal{N}(\varepsilon, S, \|\cdot\|)}{-\log \varepsilon}.$$

Given a probability measure μ on a metric space \mathcal{F} , the (ε, τ) -covering number is

$$\mathcal{N}(\varepsilon, \tau; \mu) := \inf \{ \mathcal{N}(\varepsilon, S, \|\cdot\|) : \mu(S) \geq 1 - \tau \}$$

and the (ε, τ) -dimension is

$$d(\varepsilon, \tau; \mu) := \frac{\log \mathcal{N}(\varepsilon, \tau; \mu)}{-\log \varepsilon}.$$

The upper and lower Wasserstein dimensions are respectively,

$$d_p^*(\mu) := \inf \left\{ s \in (2p, \infty) : \limsup_{\varepsilon \rightarrow 0} d(\varepsilon, \varepsilon^{\frac{s-p}{s-2p}}; \mu) \leq s \right\},$$

$$d_*(\mu) := \lim_{\tau \rightarrow 0} \liminf_{\varepsilon \rightarrow 0} d_{\varepsilon, \tau}(\mu).$$

REMARK 2.2. In the present paper, roughly speaking, $k > \max\{d_p^*(\mu), 2p\}$ will be regarded as the intrinsic dimension of μ . There is a trade off in choosing such a k to optimize the rates of convergence of empirical distributions in Wasserstein distances: see [53, Proposition 5].

We end this subsection to introduce ℓ_0 norm, which is neither norm nor even pseudo-norm but is called norm conventionally. ℓ_0 norm of X is a critical parameter of the main results. For $X = (x_1, \dots, x_d) \in \mathbb{R}^d$, the ℓ_0 norm of X is defined as

$$(2.1) \quad \|X\|_0 := \sum_{j=1}^d \mathbb{1}_{x_j \neq 0}.$$

One can understand ℓ_0 norm as the sparsity of a vector.

2.2. *Theorems.* Let $\Delta_{(d-1)}$, the $(d-1)$ -dimensional simplex, be equipped with ℓ_q distance for any $1 \leq q \leq \infty$: for $X, X' \in \Delta_{(d-1)}$

$$\text{dist}(X, X') := \|X - X'\|_q = \begin{cases} \left(\sum_{j=1}^d |x_j - x'_j|^q \right)^{\frac{1}{q}} & \text{if } 1 \leq q < \infty, \\ \max_{1 \leq j \leq d} |x_j - x'_j| & \text{if } q = \infty. \end{cases}$$

Let us recall the sequencing procedure stated in Section 1.1. Let $\mathbf{X} = \{X_1, \dots, X_n\} \subseteq \Delta_{(d-1)}$ and $\mathbf{u} = (u_1, \dots, u_n) \in \Delta_{(n-1)}$ denote the set of i.i.d. cells (samples, or gene expressions) and the (normalized) weight vector, respectively. Noisy profiles \widehat{X}_i 's follow $\widehat{X}_i \sim m_i^{-1} \text{Multinomial}(X_i, m_i)$ where $(m_1, \dots, m_n) \sim \text{Multinomial}(\mathbf{u}, m)$. If some of X_i 's are never observed, we choose $\widehat{X}_i \in \Delta_{d-1}$ arbitrarily. Finally, the noisy empirical distribution, $\widehat{\mu}_n(m)$, is obtained based on \widehat{X}_i 's.

In order to ensure that the noisy empirical distribution is a good approximation, we need the assumption on \mathbf{u} . If most u_i 's are too small, for example $u_i = O(n^{-2})$, then it is unlikely to extract gene expression from those cells so that the noisy empirical distribution cannot be close to the truth. Therefore, it should be required that most of cells can be selected according to \mathbf{u} .

ASSUMPTION 2.3. For any $n \in \mathbb{N}$, \mathbf{u} is concentrated on $\{u \in \Delta_{(n-1)} : |\{i : u_i = o(n^{-1})\}| = o(\sqrt{n \log n})\}$: more precisely, there exists a deterministic constant $c_* > 0$ independent of n such that for $n - o(\sqrt{n \log n})$ many u_i 's, it holds almost surely that

$$(2.2) \quad u_i \geq \frac{c_*}{n}.$$

The first theorem answers to question (I): given an error tolerance ϵ and n -cells, how many reads does it require to guarantee that Wasserstein distance between the noisy empirical distribution and the true empirical one is less than ϵ .

THEOREM 2.4. Fix $p \in [1, 2]$, and suppose that Theorem 2.3 holds. Then,

$$(2.3) \quad \mathbb{E}W_p(\widehat{\mu}_n(m), \mu_n) \leq \sqrt{\frac{32\mathbb{E}\|X\|_0}{c_*} \frac{n}{m}} \wedge 2 + o\left(\sqrt{\frac{\log n}{n}}\right).$$

Additionally, given $\epsilon \in (0, 1)$, $n \in \mathbb{N}$ and $\alpha \in (0, 1)$, if m satisfies

$$(2.4) \quad m \geq \frac{32(1+\alpha)n\mathbb{E}\|X\|_0}{c_*\epsilon^2} - \frac{32(1+\alpha)\epsilon^{p-2}n\mathbb{E}\|X\|_0}{c_*} \sqrt{\frac{\alpha \log n}{n}},$$

then it holds that

$$(2.5) \quad W_p(\widehat{\mu}_n(m), \mu_n) \leq \epsilon$$

with probability $1 - O(n^{-\frac{\alpha}{2}})$. The hidden constants in $O(n^{-\frac{\alpha}{2}})$ depend on α , p , $\mathbb{E}\|X\|_0$ and $\text{ess sup } \|X\|_0$.

Regarding (2.4), a lower bound of m is proportional to $\alpha, \mathbb{E}\|X\|_0, \epsilon^{-1}, c_*^{-1}, p^{-1}$ (obviously, as n larger, m should be larger). This theorem does not depend on any dimension since μ_n is an empirical distribution (discrete). Here, the most important parameter is $\mathbb{E}\|X\|_0$, the average sparsity of X . Recalling Section 1.1, if many X_i 's are sparse, then a fewer reads are sufficient to approximate them well. As n grows large, concentration phenomenon occurs so that most of $\|X_i\|_0$'s concentrate on $\mathbb{E}\|X\|_0$. For this reason, the average sparsity plays a role in order to determine a lower bound of the effective number of reads.

The inverse proportion of ϵ is usual but the dependence of c_* needs to be explained. Gene expressions of $n - o(\sqrt{n \log n})$ many cells should be measured enough to achieve (2.5). It is then necessarily satisfied that $n - o(\sqrt{n \log n})$ many cells appear during the sequencing. Unless c_* is $O(1)$, the event that $O(n)$ many cells are not observed enough would happen with non-negligible probability.

α determines the rate of the probability of the event of interest at which the probability of the event $W_p(\hat{\mu}_n(m), \mu_n) > \epsilon$ decays to 0 as $n \rightarrow \infty$. One can choose α such that it vanishes as n goes ∞ while not too fast: for example $\alpha = O\left(\frac{\log \log n}{\log n}\right)$.

Theorem 2.4 tells us that $\mathbb{E}W_p(\hat{\mu}_n(m), \mu_n) \lesssim \sqrt{\frac{n}{m}} + o\left(\sqrt{\frac{\log n}{n}}\right)$, suggesting that m needs to grow faster than n in order to obtain a diminishing Wasserstein distance between $\hat{\mu}_n(m)$ and μ_n . The following theorem provides a lower bound, confirming that this is indeed the case under certain assumptions.

THEOREM 2.5. *Let $\text{dist}(\cdot, \cdot)$ be the ℓ_q metric on $\Delta_{(d-1)}$ for $q \in [1, 2]$, and assume uniform cell weights $\mathbf{u} = (\frac{1}{n}, \dots, \frac{1}{n})$. Then for any $p \geq 1$,*

$$\mathbb{E}W_p(\hat{\mu}_n(m), \mu_n) \geq \frac{1 - \mathbb{E}\|X\|_2^2}{4} \frac{n}{m}$$

provided $\mathbb{E}\|X\|_2^2 < 1$ and $m \geq 2n \log \frac{4}{1 - \mathbb{E}\|X\|_2^2}$.

The next theorem and its corollary answer question (II), which is the main theme of this paper: given the number of m reads, how many cells can one use in order to ensure that the noisy empirical distribution is as close as possible to the true distribution μ .

Let us recall a trade-off for approximating μ in RNA sequencing: on the one hand a larger n (i.e. more cells) helps get a better approximation of μ as usual because it allows to explore the population more, but on the other hand, since m is fixed, if n is too large compared to m , gene expression of each cell cannot be measured precisely well so that the noisy empirical distribution is poorly qualified. Therefore, the optimal number of cells should be determined sophisticatedly by taking into account these contradictory aspects.

THEOREM 2.6. *Fix $\alpha \in (0, 1)$ and $p \in [1, 2]$. Assume that there are some $k > \max\{d_p^*(\mu), 2p\}$ and $m \geq m_0$ for some $m_0 = m_0(c_*, \alpha, \mathbb{E}\|X\|_0) > 0$. Let such m be fixed.*

Under Assumption 2.3, if n satisfies (2.4) given m , then $\hat{\mu}_n(m)$ satisfies

$$(2.6) \quad W_p(\hat{\mu}_n(m), \mu) \leq O\left(n^{-\frac{1}{k}}\right)$$

with probability at least $1 - O\left(n^{-\frac{\alpha}{2}}\right)$. The hidden constants in $O\left(n^{-\frac{1}{k}}\right)$ and $O\left(n^{-\frac{\alpha}{2}}\right)$ depend on k and p , and $\alpha, p, \mathbb{E}\|X\|_0$ and $\text{ess sup}\|X\|_0$, respectively.

The parameter k can be regarded as the *intrinsic dimension* of the support of μ . In reality, the intrinsic dimension k is much smaller than the ambient dimension. If the support of μ has a nice low dimensional structure, then given the same number of reads it is allowed to use more cells to approximate the population more, which helps get the noisy empirical distribution close to the truth. In other words, the low dimensional structure allows to leverage more cells to explore population more widely.

While the intrinsic dimension is unknown a priori in practice, we discuss a heuristic approximation based on the result by Block et al. [5] later in Section 3.1.3.

REMARK 2.7. One must be careful about the relation between the sparsity of X and the intrinsic dimension of μ . It is possible that even if μ has a small intrinsic dimension, X is not sparse. Suppose μ is concentrated on the diagonal, the span of $\{(1, \dots, 1)\}$. In this case $d_p^*(\mu) = 1$ but $\|X\|_0 = d$. On the other hand, however, if $\|X\|_0$ is concentrated at most $r \ll d$, then μ must exhibit a lower intrinsic dimensionality. In this sense, the sparsity of X implies a lower intrinsic dimension of μ , but the converse does not hold in general.

According to Theorem 2.6, one obtains the following corollary in a straightforward way. Here, we ignore lower order terms, and focus on the parameters of interest only. The proof is omitted.

COROLLARY 2.8. Fix $\alpha \in (0, 1)$ and $p \in [1, 2]$. Assume that there are some $k > \max\{d_p^*(\mu), 2p\}$ and $m \geq m_0$ for some $m_0 = m_0(c_*, \alpha, \mathbb{E}\|X\|_0) > 0$. Under Theorem 2.3, if n satisfies

$$(2.7) \quad n \sim \left(\frac{m}{\mathbb{E}\|X\|_0} \right)^{1 - \frac{2}{k+2}},$$

then $\hat{\mu}_n(m)$ achieves

$$(2.8) \quad W_p(\hat{\mu}_n(m), \mu) \lesssim \left(\frac{\mathbb{E}\|X\|_0}{m} \right)^{\frac{1}{k+2}}$$

with probability at least $1 - O\left(\left(\frac{m}{\mathbb{E}\|X\|_0}\right)^{-\frac{\alpha}{3}}\right)$.

It is worthwhile to mention that the order (2.8) is almost optimal. If the support of μ has the intrinsic dimension k , then $W_p(\mu_n, \mu) = O\left(n^{-\frac{1}{k}}\right)$ with high probability [53, Theorem 1, Proposition 20]. On the one hand, (2.8) yields that

$$(2.9) \quad \text{if } n \sim m^{\frac{k}{k+2}}, \text{ then } W_p(\hat{\mu}_n(m), \mu) \lesssim m^{-\frac{1}{k+2}}$$

In this sense, (2.8) achieves the almost optimal rate of convergence.

We want to emphasize that (2.8) explicitly illustrates how the sparsity and the intrinsic dimension play a role in the optimal allocation, which the previous literature did not capture. It shows that Wasserstein distance increases as k and $\mathbb{E}\|X\|_0$ increase, which perfectly coincides with our intuition. Trivially since larger k and $\mathbb{E}\|X\|_0$ require to measure more genes, the Wasserstein distance cannot but increase whenever the number of reads is fixed.

Lastly, we conclude this section by providing a lower bound on $W_p(\hat{\mu}_n(m), \mu)$, which follows directly from Theorem 2.5 and the bound $\mathbb{E}W_p(\mu_n, \mu) \leq O\left(n^{-\frac{1}{k}}\right)$ of Theorem 4.9 (Niles-Weed and Bach [53, Theorem 1]) by applying a triangle inequality twice. We omit the proof.

COROLLARY 2.9. Let $\text{dist}(\cdot, \cdot)$ be the ℓ_q metric on $\Delta_{(d-1)}$ for $q \in [1, 2]$. Let $k > \max\{d_p^*(\mu), 4\}$ and uniform cell weights $\mathbf{u} = \left(\frac{1}{n}, \dots, \frac{1}{n}\right)$. Assume further that $\mathbb{E}\|X\|_2^2 < 1$ and $m \geq 2n \log \frac{4}{1 - \mathbb{E}\|X\|_2^2}$. Then for any $p \geq 1$,

$$(2.10) \quad \mathbb{E}W_p(\hat{\mu}_n(m), \mu) \geq \max\left\{O\left(\frac{n}{m}\right), O\left(n^{-\frac{1}{k}}\right)\right\} - \min\left\{O\left(\frac{n}{m}\right), O\left(n^{-\frac{1}{k}}\right)\right\}$$

REMARK 2.10. Let $n = m^r$ and $0 < r < 1$. If the leading order of (2.10) is $n^{-\frac{1}{k}}$, then $r \leq \frac{k}{k+1}$. Similarly, if the leading order of (2.10) is $\frac{n}{m} = m^{r-1}$, $r \geq \frac{k}{k+1}$. Hence $r = \frac{k}{k+1}$ minimizes the leading order. It turns out that

$$(2.11) \quad \text{if } n \sim m^{\frac{k}{k+1}}, \text{ then } \mathbb{E}W_p(\hat{\mu}_n(m), \mu) \gtrsim m^{-\frac{1}{k+1}}.$$

Focusing on the order only, comparing (2.11) with (2.9), they almost match.

3. Empirical results.

3.1. *Experimental setup.* In this section, we empirically investigate the dependence of the optimal number of samples n^* on the sequencing budget m via simulation experiments on real single-cell datasets. Given a ground truth population distribution μ constructed from a real dataset, we generate n i.i.d. samples followed by m reads for various values of n and m , yielding noisy empirical distributions $\hat{\mu}_n(m)$ (recall the sampling and sequencing procedures from Section 2.1). The resulting Wasserstein errors $W_1(\hat{\mu}_n(m), \mu)$ then reveal the desired dependence, demonstrating the validity of our theoretical results from Section 2.2. Throughout this section, we use the ℓ_1 distance on the simplex $\Delta_{(d-1)}$ as our ground metric in computing W_1 .

3.1.1. *Datasets.* We focus on a subset of the scRNA-seq *cellular reprogramming* dataset from Schiebinger et al. [65] in this section – particularly cells from the D15.5 Serum timepoints. Results from similar experiments on two additional datasets – the *sea urchin* dataset [47] and the *Arabidopsis* dataset [66] – are deferred to Section A. Further details about the specific data files and preprocessing tools are presented in Section B.1.

Each dataset here is available as a cells-by-genes counts matrix of reads recorded in sequencing experiments (more precisely, unique molecular identifier (UMI) reads [39]). Denote this matrix as

$$\mathbf{C} = \begin{bmatrix} - & C_1^T & - \\ & \vdots & \\ - & C_N^T & - \end{bmatrix} \in \mathbb{N}_0^{N \times d},$$

whose rows correspond to the N cells measured. Note that although this matrix was obtained experimentally, which necessarily corresponds to an ‘empirical’ distribution in reality, we treat it as the ground truth population in our simulations. Particularly, we construct the distribution μ as

$$(3.1) \quad \mu = \frac{1}{N} \sum_{\ell=1}^N \delta_{C_\ell / \|C_\ell\|_1} \in \mathcal{P}(\Delta_{(d-1)}).$$

Note that μ defined in such a manner is an atomic measure; its discrete nature enables easy generation of (pseudorandom) samples and computation of Wasserstein distances $W_1(\hat{\mu}_n(m), \mu)$. For μ constructed from the *reprogramming* dataset considered in this section, we have $d = 1000$, $N = 4851$ and $\mathbb{E}P_{\sim\mu}\|X\|_0 \simeq 175$.

3.1.2. *Cell weights.* Recall that the noisy sequencing process stated in Section 1.1 depends on the normalized cell weights $\mathbf{u} = (u_1, \dots, u_n) \in \Delta_{n-1}$, which, as discussed earlier, may or may not be independent of the gene expression vectors $\{X_1, \dots, X_n\}$. A simple scenario is that of uniform cell weights $\mathbf{u} = (\frac{1}{n}, \dots, \frac{1}{n})$, which we investigate first (Section 3.2, Section 3.3). A general formulation considers the joint distribution $(X, U) \sim \mu_{(X,U)}$, and this is studied in Section 3.4.

3.1.3. *Assessing the intrinsic dimension.* The theoretical results from Section 2.2 depend on the intrinsic dimension k (related to the upper Wasserstein dimension) of μ (see Theorem 2.1 and Theorem 2.2). Because the Wasserstein dimensions can be hard to compute in practice, we rely on a heuristic approximation following the results of Niles-Weed and Bach [53] and ideas from Block et al. [5]. Noting that sufficiently regular probability measures μ display

$$\Omega(n^{-1/k}) \leq \mathbb{E} W_1(\mu, \mu_n) \leq O(n^{-1/\bar{k}})$$

(where μ_n is the n -sample (true) empirical distribution) for any $k < d_*(\mu) = d^*(\mu) < \bar{k}$, one can use the rate of decay of $\mathbb{E} W_1(\mu, \mu_n)$ to estimate k . More precisely, for various values of n , we repeatedly draw i.i.d. samples from μ to form μ_n , and compute $W_1(\mu, \mu_n)$ for each such trial. Then, we fit a straight line to the resulting set of pairs $(\log n, \log W_1(\mu, \mu_n))$, the slope of which approximates $-1/k$. For the reprogramming dataset, this procedure gives $k = 9.718$ (which is much smaller than the ambient dimension $d = 1000$); see Section B.2 and Figure 7.

In Section 3.3 below, we conduct tests on lower-dimensional versions of μ , with various intrinsic dimensions k , that we construct via non-negative matrix factorization of the normalized counts matrix.

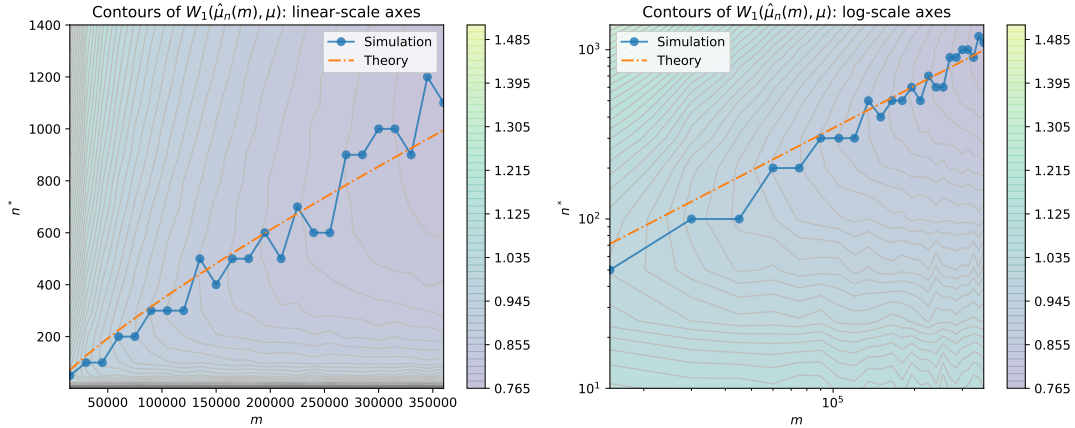


FIGURE 2. **Optimal allocation (m - n relationship) with uniform cell weights.** The contours and the colour scale show $W_1(\hat{\mu}_n(m), \mu)$ averaged over ten (10) independent realizations of $\hat{\mu}_n(m)$, for various pairs of m and n on a grid. The m and n axes are plotted in a linear scale on the left panel, and in a log scale on the right panel. The optimal values of n^* for each m , as observed in this simulation, are plotted with blue solid dots. Our theoretically derived optimal allocation, with estimated intrinsic dimension $k = 9.718$

, is plotted as an orange dash-dot line.

3.2. *Results on the reprogramming dataset with uniform cell weights.* For various pairs of n and m , we simulate the noisy empirical distribution $\hat{\mu}_n(m)$ for ten (10) independent trials, and compute the mean Wasserstein error $W_1(\hat{\mu}_n(m), \mu)$ over those trials. Contours of mean $W_1(\hat{\mu}_n(m), \mu)$ over m - n axes are plotted in Figure 2. For each budget m tested, we identify the number of cells $n = n^*$ that yields the lowest mean $W_1(\hat{\mu}_n(m), \mu)$. This m - n^* relationship, shown in Figure 2, appears to be well captured by our theoretically derived optimal allocation (from Theorem 2.8)

$$(3.2) \quad n \sim \left(\frac{Cm}{\mathbb{E}\|X\|_0} \right)^{1 - \frac{2}{2+k}}$$

where C is a $\Theta(1)$ constant. We have used the value $C = 2$ in the figure. The exponent $1 - \frac{2}{2+k}$ shows up as the slope on the log-scale plot in Figure 2 (right panel).

3.3. Results for various intrinsic dimensions. The optimal allocation is crucially dependent on the intrinsic dimension k . We investigate this further by constructing synthetic versions of the reprogramming dataset with different values of k to produce synthetic population distributions μ_k . Details on these constructions, and some statistics of the synthetic datasets, are presented in Section B.3. As before, the intrinsic dimensions in question are estimated via the heuristic from Section 3.1.3; see Figure 8.

We repeat the experiment from Section 3.2 on the synthetic distributions μ_k for various values of k ; the observed $\log m - \log n^*$ relationships are presented in Figure 3. For a more quantitative assessment, we estimate the slope of each observed $\log m - \log n^*$ relationship via a linear least squares fit (green dash-dot line), and track its dependence on k . The optimal allocation theory (3.2) suggests that this slope be $1 - \frac{2}{k+2}$ (orange dash-dot line). We set $C = 2$ as in Section 3.2.

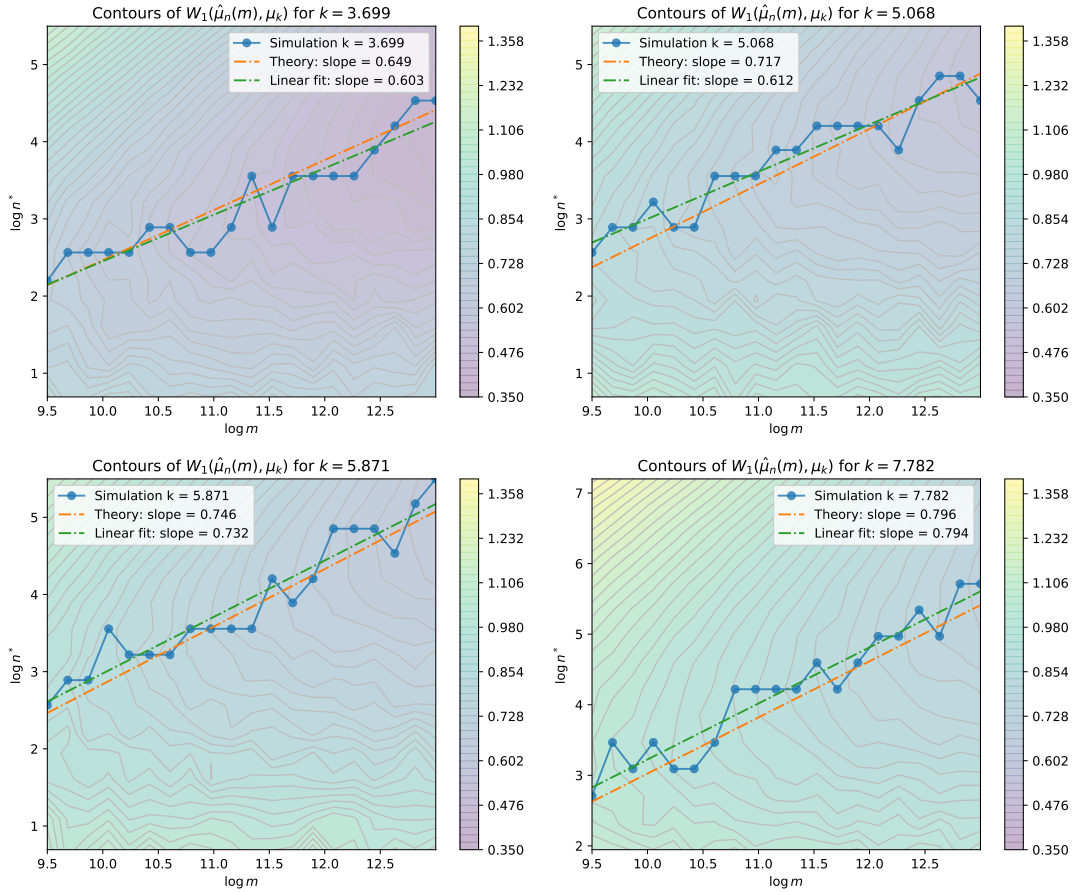


FIGURE 3. **Optimal allocations for different intrinsic dimensions k .** Each panel shows the optimal allocation results for a synthetic population distribution μ_k of a different intrinsic dimension k . The contours and the color scale show $W_1(\hat{\mu}_n(m), \mu_k)$ averaged over ten (10) independent realizations of $\hat{\mu}_n(m)$, for various pairs of m and n . The optimal values $\log n^*$ for each $\log m$, as observed in the simulations, are plotted with blue solid dots. Linear least squares fits to these $\log m - \log n^*$ relationships are plotted as green dash-dot lines. Finally, our theoretically derived optimal allocations are plotted as orange dash-dot lines.

We notice that the theory predicts the fitted slopes fairly well across the values of k tested. Moreover, the different slopes observed in Figure 3, which are smaller than 1 in particular, demonstrate variably sublinear dependence of n^* on m ; this is different from the linear relationship discussed in Zhang, Ntranos and Tse [82].

3.4. Results in the case of non-uniform cell weights. To simulate sequencing with general, non-uniform cell weights, we construct the ground truth distribution $\mu_{(X,U)}$ from real data as before. Since the number of reads that a cell receives is an indication of its sampling frequency, we can use the row sums of \mathbf{C} to help construct $\mu_{(X,U)}$. In order to capture the possible dependence or independence between X and U , two scenarios are considered in our experiments.

Scenario 1. U dependent on X . Here, we always match a sampled cell to its original weight in the ground truth counts matrix \mathbf{C} . More precisely,

$$\mu_{(X,U)} = \frac{1}{N} \sum_{\ell=1}^N \delta_{(C_\ell / \|C_\ell\|_1, \|C_\ell\|_1)}.$$

Scenario 2. U independent of X . Here, a sampled cell is paired with an independently chosen weight from the ground truth counts matrix \mathbf{C} :

$$\mu_{(X,U)} = \frac{1}{N^2} \sum_{\ell,k=1}^N \delta_{(C_\ell / \|C_\ell\|_1, \|C_k\|_1)}.$$

Note that the two scenarios only differ in their couplings of X and U ; the marginals of X and U remain the same. The X -marginal in both cases equals μ as defined in (3.1).

Our optimal allocation theory is agnostic to the possible dependence between X and U , and we verify that this is also the case in simulations. We repeat the experiment from Section 3.2 under scenarios 1 and 2, and present the results in Figure 4 and Figure 5 respectively. The behavior is similar to that seen in Figure 2; the observed m - n^* relationships are quite close to the theoretically derived optimal allocations (3.2), with $C = 4/3$.

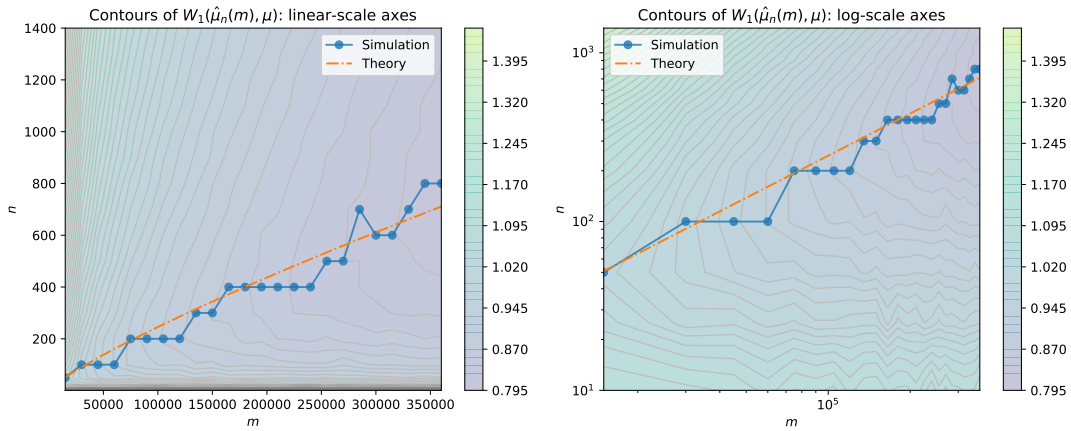


FIGURE 4. **Optimal allocation with non-uniform cell weights: Scenario 1 (U dependent on X).** The contours and the colour scale show $W_1(\hat{\mu}_n(m), \mu)$ averaged over ten (10) independent realizations of $\hat{\mu}_n(m)$, for various pairs of m and n . The m and n axes are plotted in a linear scale on the left panel, and in a log scale on the right panel. The optimal values of n^* for each m , as observed in this simulation, are plotted with blue solid dots. Our theoretically derived optimal allocation with estimated intrinsic dimension $k = 9.718$, is plotted as an orange dash-dot line.

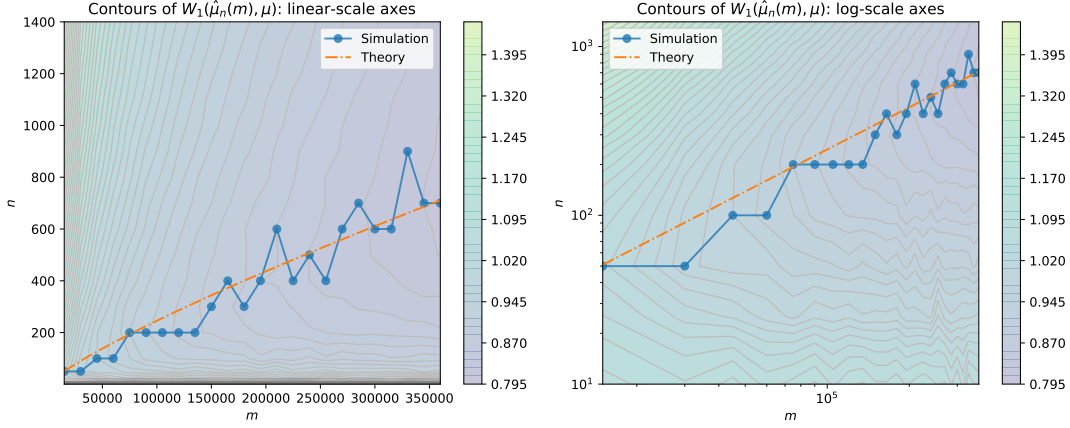


FIGURE 5. **Optimal allocation with non-uniform cell weights: Scenario 2 (U independent of X).** The contours and the colour scale show $W_1(\hat{\mu}_n(m), \mu)$ averaged over ten (10) independent realizations of $\hat{\mu}_n(m)$, for various pairs of m and n . The m and n axes are plotted in a linear scale on the left panel, and in a log scale on the right panel. The optimal values of n^* for each m , as observed in this simulation, are plotted with blue solid dots. Our theoretically derived optimal allocation with estimated intrinsic dimension $k = 9.718$, is plotted as an orange dash-dot line.

4. Proofs. Let's recall the problem setting. $\mathbf{X} := \{X_1, \dots, X_n\} \subseteq \Delta_{(d-1)}$ and $\mathbf{u} = (u_1, \dots, u_n) \in \Delta_{(n-1)}$ denote the set of gene expressions of n -cells and the vector of the weight vector of cells, respectively, and μ is the unknown ground truth distribution. A true empirical distribution and the noisy one are denoted by

$$\mu_n := \sum_{i=1}^n \frac{1}{n} \delta_{X_i} \text{ and } \hat{\mu}_n(m) := \sum_{i=1}^n \frac{1}{n} \delta_{\hat{X}_i},$$

respectively.

4.1. *Proof of Theorem 2.4.* The first objective is to control $W_p(\hat{\mu}_n(m), \mu_n)$. The following lemma allows to bound $W_p(\hat{\mu}_n(m), \mu_n)$ by $\left(\sum \text{dist}(\hat{X}_i, X_i)^p\right)^{\frac{1}{p}}$.

LEMMA 4.1. [76, Theorem 4.8] *Let \mathcal{X} and \mathcal{Y} be Polish spaces, and $c : \mathcal{X} \times \mathcal{Y} \rightarrow \mathbb{R} \cup \{\infty\}$ be a lower semicontinuous function. For each $\mu \in \mathcal{P}(\mathcal{X})$ and $\nu \in \mathcal{P}(\mathcal{Y})$*

$$C(\mu, \nu) := \inf_{\pi \in \Pi(\mu, \nu)} \int_{\mathcal{X} \times \mathcal{Y}} c(x, y) d\pi(x, y),$$

the associated optimal transport cost functional. Let (Θ, λ) be a probability space, and let μ_θ, ν_θ be two measurable probability measures on $\mathcal{P}(\mathcal{X})$ and $\mathcal{P}(\mathcal{Y})$, respectively. Assume that $c(x, y) \geq a(x) + b(y)$, where $a \in L^1(d\mu_\theta d\lambda(\theta))$ and $b \in L^1(d\nu_\theta d\lambda(\theta))$. Then,

$$C\left(\int_{\Theta} \mu_\theta d\lambda(\theta), \int_{\Theta} \nu_\theta d\lambda(\theta)\right) \leq \int_{\Theta} C(\mu_\theta, \nu_\theta) d\lambda(\theta).$$

Theorem 4.1 states the convexity of optimal transport functional. Since norms over \mathbb{R}^d are lower semicontinuous, Jensen's inequality implies that W_p for any $p \geq 1$ enjoys convexity. More precisely,

$$W_p^p(\hat{\mu}_n(m), \mu_n) \leq \sum_{i=1}^n \frac{1}{n} W_p^p(\delta_{\hat{X}_i}, \delta_{X_i}) = \sum_{i=1}^n \frac{1}{n} \text{dist}(\hat{X}_i, X_i)^p.$$

Hence, one gets

$$(4.1) \quad W_p(\widehat{\mu}_n(m), \mu_n) \leq \left(\sum_{i=1}^n \frac{1}{n} \text{dist}(\widehat{X}_i, X_i)^p \right)^{\frac{1}{p}}.$$

Therefore, the problem reduces to achieving $\sum \frac{1}{n} \text{dist}(\widehat{X}_i, X_i)^p$ to be small with high probability.

$\sum \frac{1}{n} \text{dist}(\widehat{X}_i, X_i)^p$ would be small by concentration phenomenon if n is large, and also m is large enough proportional to n . The concentration inequality of the empirical estimator of the event probability vector of multinomial distribution is well-known. The next lemma is regarding the concentration inequality of it. Originally, Weissman et al. [80, Theorem 2.1] concern only ℓ_1 norm. However, since $\|X - X'\|_1 \geq \|X - X'\|_q$ holds on $\Delta_{(d-1)}$ for any $1 \leq q \leq \infty$, one can extend the concentration inequality to ℓ_q norms. Recalling the ℓ_0 norm defined in (2.1), the concentration inequality depends on an error parameter δ and $\|X\|_0$ and the number of iteration m .

LEMMA 4.2. [80, Theorem 2.1][60, Proposition 1] Let $X \in \Delta_{(d-1)}$ and $\widehat{X} = \widehat{X}(m)$ be the empirical estimator of X with m trials. Then, for any $\delta \in [0, 1]$ and $p \in [1, \infty)$,

$$(4.2) \quad \mathbb{P} \left(\text{dist}(\widehat{X}, X)^p \leq \left(\frac{2\|X\|_0 \log(\frac{1}{\delta})}{m} \right)^{\frac{p}{2}} \right) \geq 1 - \delta.$$

Let $\epsilon \in (0, 1)$ be the fixed error tolerance. Recall Section 1.1 that

$$(4.3) \quad \mathbf{m} \sim \text{Multinomial}(\mathbf{u}, m)$$

where $\mathbf{m} := (m_1, \dots, m_n)$ is a multinomial vector over n integer with m trials and an event probability vector \mathbf{u} . Restricting to a single i , each marginal m_i follows binomial distribution with m trials and a success probability u_i .

Let $\alpha_i := \exp\left(-\frac{m_i \epsilon^2}{2\|X_i\|_0}\right)$. (4.2) leads to for each i and $k \in \{1, \dots, \lfloor \frac{2^p}{\epsilon^p} \rfloor\}$

$$\mathbb{P} \left(\text{dist}(\widehat{X}_i, X_i)^p \geq k\epsilon^p \mid \mathbf{m}, \mathbf{X}, \mathbf{u} \right) \leq \alpha_i^{k^{\frac{2}{p}}}.$$

In particular,

$$\mathbb{P} \left((k-1)\epsilon^p \leq \text{dist}(\widehat{X}_i, X_i)^p < k\epsilon^p \mid \mathbf{m}, \mathbf{X}, \mathbf{u} \right) \leq \alpha_i^{(k-1)^{\frac{2}{p}}} - \alpha_i^{k^{\frac{2}{p}}}.$$

Here α_i is a random variable depending on m_i , \mathbf{X} and \mathbf{u} . Notice that $\text{dist}(\widehat{X}_i, X_i)^p \leq 2^p$ almost surely.

A next lemma is regarding the construction of a new analyzable random variable Z_i which stochastically dominates $\text{dist}(\widehat{X}_i, X_i)^p$. Stochastic dominance is frequently used in various fields including finance, economics, statistics and etc. in order to measure uncertainty among several random variables(vectors). Among many variants of it, here we rely on the first order stochastic dominance.

DEFINITION 4.3. [62, Definition 4.2.1] Let μ and ν be probability measures on \mathbb{R} . The measure μ is said to stochastically dominate ν if for all $x \in \mathbb{R}$,

$$\mu((x, \infty)) \geq \nu((x, \infty)).$$

A real random variable X stochastically dominates Y if the law of X dominates the law of Y .

LEMMA 4.4. For each $1 \leq i \leq n$ define a random variable Z_i which takes a value $\{\epsilon^p, \dots, \lfloor \frac{2^p}{\epsilon^p} \rfloor \epsilon^p, 2^p\}$ as

$$(4.4) \quad \mathbb{P}(Z_i = k\epsilon^p \mid \mathbf{m}, \mathbf{X}, \mathbf{u}) = \begin{cases} \alpha_i^{(k-1)\frac{2}{p}} - \alpha_i^{k\frac{2}{p}} & \text{if } k = 1, \dots, \lfloor \frac{2^p}{\epsilon^p} \rfloor, \\ \alpha_i^{\lfloor \frac{2^p}{\epsilon^p} \rfloor \frac{2}{p}} & \text{if } k = \frac{2^p}{\epsilon^p}. \end{cases}$$

Then Z_i stochastically dominates $\text{dist}(\widehat{X}_i, X_i)^p$ conditioned on $\mathbf{m}, \mathbf{X}, \mathbf{u}$.

PROOF. One needs to show that for any $t \in [0, 2^p]$

$$\mathbb{P}(Z_i \geq t \mid \mathbf{m}, \mathbf{X}, \mathbf{u}) \geq \mathbb{P}(\text{dist}(\widehat{X}_i, X_i)^p \geq t \mid \mathbf{m}, \mathbf{X}, \mathbf{u})$$

and the strict inequality holds for some t unless the distribution of $\text{dist}(\widehat{X}_i, X_i)^p$ is equal to that of Z_i conditioned on $\mathbf{m}, \mathbf{X}, \mathbf{u}$. From (4.2) and (4.4), for $t \in ((k-1)\epsilon^p, k\epsilon^p)$ it is straightforward that

$$\begin{aligned} \mathbb{P}(\text{dist}(\widehat{X}_i, X_i)^p \geq t \mid \mathbf{m}, \mathbf{X}, \mathbf{u}) &\leq \mathbb{P}(\text{dist}(\widehat{X}_i, X_i)^p \geq (k-1)\epsilon^p \mid \mathbf{m}, \mathbf{X}, \mathbf{u}) \\ &\leq \alpha_i^{(k-1)\frac{2}{p}} \\ &= \mathbb{P}(Z_i \geq (k-1)\epsilon^p \mid \mathbf{m}, \mathbf{X}, \mathbf{u}). \end{aligned}$$

□

It is immediate that $\sum Z_i$ stochastically dominates $\sum \text{dist}(\widehat{X}_i, X_i)^p$ by the following lemma.

LEMMA 4.5. [62, Corollary 4.2.7] If X_i stochastically dominates Y_i for $i = 1, 2$, then $X_1 + X_2$ stochastically dominates $Y_1 + Y_2$.

One advantage of the construction of Z_i 's is that it is easy to compute an upper bound of the expectation of Z_i .

LEMMA 4.6. Let Z_i be the random variable defined in Theorem 4.4 for fixed $p \in [1, 2]$. Then,

$$(4.5) \quad \mathbb{E}[Z_i \mid \mathbf{X}, \mathbf{u}] \leq \begin{cases} \left(\epsilon^{p-2} \frac{32\|X_i\|}{u_i m} \right) \wedge 2^p & \text{if } m < \frac{16\|X_i\|_0}{u_i \epsilon^2}, \\ \left(\frac{\epsilon^p}{1-\epsilon^{-2}} \right) \wedge 2^p & \text{if } m \geq \frac{16\|X_i\|_0}{u_i \epsilon^2} \end{cases}$$

Here, $x \wedge y := \min\{x, y\}$.

PROOF. Recall $\alpha_i := \exp\left(-\frac{m_i \epsilon^2}{2\|X_i\|_0}\right)$. A straightforward calculation yields

$$\begin{aligned} \mathbb{E}[Z_i \mid \mathbf{m}, \mathbf{X}, \mathbf{u}] &= \sum_{k=1}^{\lfloor \frac{2^p}{\epsilon^p} \rfloor} k\epsilon^p \left(\alpha_i^{(k-1)\frac{2}{p}} - \alpha_i^{k\frac{2}{p}} \right) + 2^p \alpha_i^{\lfloor \frac{2^p}{\epsilon^p} \rfloor \frac{2}{p}} \\ &= \epsilon^p - \epsilon^p \alpha_i + 2\epsilon^p \alpha_i - 2\epsilon^p \alpha_i^{\frac{2}{p}} + 3\epsilon^p \alpha_i^{\frac{2}{p}} - 3\epsilon^p \alpha_i^{\frac{3}{p}} + \dots + 2^p \alpha_i^{\lfloor \frac{2^p}{\epsilon^p} \rfloor \frac{2}{p}} \\ &\leq \epsilon^p \sum_{k=0}^{\lfloor \frac{2^p}{\epsilon^p} \rfloor} \alpha_i^{k\frac{2}{p}}. \end{aligned}$$

Let $\gamma_i := \exp\left(-\frac{\epsilon^2}{2\|X_i\|_0}\right)$ for simplicity. Since each m_i is a binomial random variable with parameters m and u_i , it follows from the moment generating function of m_i that

$$\begin{aligned}\mathbb{E}[\alpha_i^{k^{\frac{2}{p}}} | \mathbf{X}, \mathbf{u}] &= \mathbb{E}[(\gamma_i^{k^{\frac{2}{p}}})^{m_i} | \mathbf{X}, \mathbf{u}] = ((1 - u_i) + u_i \gamma_i^{k^{\frac{2}{p}}})^m \\ &= [(1 - (1 - \gamma_i^{k^{\frac{2}{p}}})u_i)]^m \leq \exp(-u_i m (1 - \gamma_i^{k^{\frac{2}{p}}}),\end{aligned}$$

where we used the fact that $(1 - \gamma_i^{k^{\frac{2}{p}}})u_i \leq 1$ along with the elementary inequality $1 - x \leq \exp(-x)$ for $x \in \mathbb{R}$.

We study the term $\gamma_i^{k^{\frac{2}{p}}} = \exp\left(-\frac{k^{\frac{2}{p}}\epsilon^2}{2\|X_i\|_0}\right)$ further. Noting $k \leq \frac{2^p}{\epsilon^p}$ in the sum above, we have

$$\frac{k^{\frac{2}{p}}\epsilon^2}{2\|X_i\|_0} \leq \frac{2^2}{\epsilon^2} \frac{\epsilon^2}{2\|X_i\|_0} = \frac{2}{\|X_i\|_0} \leq 2,$$

since $\|X\|_0 \geq 1$ for any $X \in \Delta_{(d-1)}$. By convexity of $\exp(\cdot)$, we have that for any $x \in [0, 2]$,

$$(*) \quad \exp(-x) \leq 1 - \frac{1 - e^{-2}}{2}x \leq 1 - \frac{x}{4}.$$

As a result, we obtain the bound

$$1 - \gamma_i^{k^{\frac{2}{p}}} = 1 - \exp\left(-\frac{k^{\frac{2}{p}}\epsilon^2}{2\|X_i\|_0}\right) \geq \frac{k^{\frac{2}{p}}\epsilon^2}{8\|X_i\|_0}$$

which finally gives

$$\mathbb{E}\left[\alpha_i^{k^{\frac{2}{p}}} | \mathbf{X}, \mathbf{u}\right] \leq \exp\left(-u_i m \left(1 - \gamma_i^{k^{\frac{2}{p}}}\right)\right) \leq \exp\left(-\frac{u_i m \epsilon^2}{8\|X_i\|_0} k^{\frac{2}{p}}\right).$$

Thus, an upper bound of the conditional expectation of Z_i is derived as

$$\begin{aligned}\mathbb{E}[Z_i | \mathbf{X}, \mathbf{u}] &\leq \epsilon^p \sum_{k=0}^{\lfloor \frac{2^p}{\epsilon^p} \rfloor} \mathbb{E}\left[\alpha_i^{k^{\frac{2}{p}}} | \mathbf{X}, \mathbf{u}\right] \\ &\leq \epsilon^p \sum_{k=0}^{\lfloor \frac{2^p}{\epsilon^p} \rfloor} \exp\left(-\frac{u_i m \epsilon^2}{8\|X_i\|_0} k^{\frac{2}{p}}\right) \\ &\leq \epsilon^p \sum_{k=0}^{\lfloor \frac{2^p}{\epsilon^p} \rfloor} \exp\left(-\frac{u_i m \epsilon^2}{8\|X_i\|_0} k\right) \quad (\text{because } p \in [1, 2]) \\ &\leq \epsilon^p \sum_{k=0}^{\infty} \exp\left(-\frac{u_i m \epsilon^2}{8\|X_i\|_0} k\right) \\ &\leq \frac{\epsilon^p}{1 - \exp\left(-\frac{u_i m \epsilon^2}{8\|X_i\|_0}\right)}.\end{aligned}$$

If $m < \frac{16\|X_i\|_0}{u_i \epsilon^2}$, i.e., $\frac{u_i m \epsilon^2}{8\|X_i\|_0} \leq 2$, by applying (*) again to the last line, one gets

$$\frac{\epsilon^p}{1 - \exp\left(-\frac{u_i m \epsilon^2}{8\|X_i\|_0}\right)} \leq \epsilon^{p-2} \frac{32\|X_i\|_0}{u_i m}.$$

Otherwise, if $m \geq \frac{16\|X_i\|_0}{u_i\epsilon^2}$, since $1 - \exp\left(-\frac{u_i m \epsilon^2}{8\|X_i\|_0}\right) \geq 1 - e^{-2}$, one gets

$$\frac{\epsilon^p}{1 - \exp\left(-\frac{u_i m \epsilon^2}{8\|X_i\|_0}\right)} \leq \frac{\epsilon^p}{(1 - e^{-2})}.$$

The fact that $Z_i \leq 2^p$, on the other hand, trivially gives $\mathbb{E}[Z_i \mid \mathbf{X}, \mathbf{u}] \leq 2^p$. \square

Combining Lemmas 4.4 and 4.5, we get

$$(4.6) \quad \mathbb{P}\left(\frac{1}{n} \sum_{i=1}^n \text{dist}(\widehat{X}_i, X_i)^p \geq t \mid \mathbf{m}, \mathbf{X}, \mathbf{u}\right) \leq \mathbb{P}\left(\frac{1}{n} \sum_{i=1}^n Z_i \geq t \mid \mathbf{m}, \mathbf{X}, \mathbf{u}\right).$$

Although the expectations of $\text{dist}(\widehat{X}_i, X_i)$'s are complicated, we now know an upper bound of the expectations of Z_i 's. Hence, the strategy that we adopt is to derive the concentration inequality of the sum of Z_i 's by using (4.5). Then combined with (4.6), the concentration will give a lower bound of m given n to achieve the error rate at most ϵ .

Recalling (4.5), notice that if $m \geq \frac{16\sum_{i=1}^n \|X_i\|_0}{c_*\epsilon^2}$,

$$\frac{32\epsilon^{p-2}}{c_*m} \sum_{u_i: u_i \geq \frac{c_*}{n}} \|X_i\|_0 \leq 2\epsilon^p.$$

Hence paying a multiplicative factor at most 2, from Theorem 2.3 and (4.5), an upper bound of the conditional expectation of the sum of Z_i 's is derived as

$$(4.7) \quad \mathbb{E}\left[\frac{1}{n} \sum_{i=1}^n Z_i \mid \mathbf{X}, \mathbf{u}\right] \leq \left(\frac{32\epsilon^{p-2}}{c_*m} \sum_{u_i: u_i \geq \frac{c_*}{n}} \|X_i\|_0\right) \wedge 2^p + o\left(\sqrt{\frac{\log n}{n}}\right)$$

for all $m \geq 0$. Thus, for any fixed $\epsilon \in (0, 1)$, (4.7) turns out to be

$$\mathbb{E}\left[\frac{1}{n} \sum_{i=1}^n Z_i \mid \mathbf{X}, \mathbf{u}\right] \leq \epsilon^p + o\left(\sqrt{\frac{\log n}{n}}\right)$$

if m satisfies

$$m \geq \frac{32\sum_{i=1}^n \|X_i\|_0}{c_*\epsilon^2}.$$

To obtain a deterministic lower bound of m , we take advantage of the fact that $\sum_{i=1}^n \|X_i\|_0$ also exhibits a concentration phenomenon.

LEMMA 4.7. *Fix $\alpha \in (0, 1)$. Then,*

$$(4.8) \quad \mathbb{P}\left(\sum_{i=1}^n \|X_i\|_0 \geq (1 + \alpha)n\mathbb{E}\|X\|_0\right) \leq \exp\left(-\frac{2\alpha^2(\mathbb{E}\|X\|_0)^2 n}{\text{ess sup } \|X\|_0}\right).$$

PROOF. Notice that each $\|X_i\|_0$ is bound from 0 to d . Let c_j be the maximum value of the j -th entry of X . Since $c_j \leq 1$, (2.1) leads to μ -almost surely

$$\sum_{j=1}^d c_j^2 \leq \sup\left\{\sum_{j=1}^d \mathbb{1}_{x_j \neq 0} : \mu(\{X \in \Delta_{(d-1)} : \sum_{j=1}^d \mathbb{1}_{x_j \neq 0} > 0\}) > 0\right\} = \text{ess sup } \|X\|_0.$$

Using Hoeffding's inequality or McDiarmid's inequality straightforwardly with the above bound implies that

$$\mathbb{P} \left(\sum_{i=1}^n \|X_i\|_0 - \mathbb{E} \sum_{i=1}^n \|X_i\|_0 \geq t \right) \leq \exp \left(-\frac{2t^2}{n \operatorname{ess\,sup} \|X\|_0} \right).$$

Fix $\alpha \in (0, 1)$. Choosing $t = \alpha \mathbb{E} \sum_{i=1}^n \|X_i\|_0 = \alpha n \mathbb{E} \|X\|_0$, it follows that

$$\mathbb{P} \left(\sum_{i=1}^n \|X_i\|_0 \geq (1 + \alpha)n \mathbb{E} \|X\|_0 \right) \leq \exp \left(-\frac{2\alpha^2 (\mathbb{E} \|X\|_0)^2 n}{\operatorname{ess\,sup} \|X\|_0} \right).$$

□

REMARK 4.8. Since $\frac{(\mathbb{E} \|X\|_0)^2}{\operatorname{ess\,sup} \|X\|_0}$ does not depend on n , the right hand side of (4.8) decays as $n \rightarrow \infty$.

Now, we are ready to prove Theorem 2.4.

PROOF OF THEOREM 2.4. A direct consequence of (4.7) is that under Theorem 2.3,

$$\mathbb{E} \left[\frac{1}{n} \sum_{i=1}^n Z_i \right] \leq \left(\frac{32\epsilon^{p-2} n \mathbb{E} \|X\|_0}{c_* m} \right) \wedge 2^p + o \left(\sqrt{\frac{\log n}{n}} \right).$$

Setting $\epsilon^2 = \frac{32n \mathbb{E} \|X\|_0}{c_* m}$, and noting that

$$\mathbb{E} W_p(\hat{\mu}_n(m), \mu_n) \leq (\mathbb{E} W_p^p(\hat{\mu}_n(m), \mu_n))^{\frac{1}{p}} \leq \left(\mathbb{E} \left[\frac{1}{n} \sum_{i=1}^n Z_i \right] \right)^{\frac{1}{p}}$$

concludes the bound in expectation (2.3).

If m satisfies (2.4), combining (4.7) with (4.8), it follows that

$$\mathbb{E} \left[\frac{1}{n} \sum_{i=1}^n Z_i \mid \mathbf{X}, \mathbf{u} \right] \leq \epsilon^p - \sqrt{\frac{\alpha \log n}{n}} + o \left(\sqrt{\frac{\log n}{n}} \right).$$

Notice that this upper bound is independent of \mathbf{X} and \mathbf{u} . Therefore, if m satisfies (2.4), then

$$(4.9) \quad \mathbb{E} \left[\frac{1}{n} \sum_{i=1}^n Z_i \right] = \mathbb{E} \left[\mathbb{E} \left[\frac{1}{n} \sum_{i=1}^n Z_i \mid \mathbf{X}, \mathbf{u} \right] \right] \leq \epsilon^p - \sqrt{\frac{\alpha \log n}{n}} + o \left(\sqrt{\frac{\log n}{n}} \right).$$

To obtain an upper bound of the tail probability of $\frac{1}{n} \sum Z_i$, since $Z_i \in [0, 2^p]$ almost surely, applying Hoeffding's inequality with (4.9) leads to

$$\begin{aligned} & \mathbb{P} \left(\frac{1}{n} \sum_{i=1}^n Z_i \geq \epsilon^p \right) \\ &= \mathbb{P} \left(\frac{1}{n} \sum_{i=1}^n Z_i - \mathbb{E} \left[\frac{1}{n} \sum_{i=1}^n Z_i \right] \geq \epsilon^p - \mathbb{E} \left[\frac{1}{n} \sum_{i=1}^n Z_i \right] \right) \\ &\leq \mathbb{P} \left(\frac{1}{n} \sum_{i=1}^n Z_i - \mathbb{E} \left[\frac{1}{n} \sum_{i=1}^n Z_i \right] \geq \sqrt{\frac{\alpha \log n}{n}} - o \left(\sqrt{\frac{\log n}{n}} \right) \mid \sum_{i=1}^n \|X_i\|_0 \leq (1 + \alpha)n \mathbb{E} \|X\|_0 \right) \end{aligned}$$

$$\begin{aligned}
& \times \mathbb{P} \left(\sum_{i=1}^n \|X_i\|_0 \leq (1 + \alpha)n\mathbb{E}\|X\|_0 \right) + \mathbb{P} \left(\sum_{i=1}^n \|X_i\|_0 \geq (1 + \alpha)n\mathbb{E}\|X\|_0 \right) \\
& \leq \exp \left(- \frac{n \left(\sqrt{\frac{\alpha \log n}{n}} - o \left(\sqrt{\frac{\log n}{n}} \right) \right)^2}{2^{2p-1}} \right) \left(1 - \exp \left(- \frac{2\alpha^2(\mathbb{E}\|X\|_0)^2 n}{\text{ess sup } \|X\|_0} \right) \right) \\
& \quad + \exp \left(- \frac{2\alpha^2(\mathbb{E}\|X\|_0)^2 n}{\text{ess sup } \|X\|_0} \right) \\
& \leq O \left(n^{-\frac{\alpha}{2}} \right).
\end{aligned}$$

Combining this with the stochastic domination relation (4.6), it follows that if m satisfies (2.4),

$$\begin{aligned}
\mathbb{P} \left(\frac{1}{n} \sum_{i=1}^n \text{dist}(\widehat{X}_i, X_i) \geq \epsilon^p \right) &= \mathbb{E} \left[\mathbb{P} \left(\frac{1}{n} \sum_{i=1}^n \text{dist}(\widehat{X}_i, X_i) \geq \epsilon^p \mid \mathbf{m}, \mathbf{X}, \mathbf{u} \right) \right] \\
&\leq \mathbb{E} \left[\mathbb{P} \left(\frac{1}{n} \sum_{i=1}^n Z_i \geq \epsilon^p \mid \mathbf{m}, \mathbf{X}, \mathbf{u} \right) \right] \\
&= \mathbb{P} \left(\frac{1}{n} \sum_{i=1}^n Z_i \geq \epsilon^p \right) \\
&\leq O \left(n^{-\frac{\alpha}{2}} \right).
\end{aligned}$$

Therefore, the conclusion follows from (4.1). \square

4.2. *Proof of Theorem 2.5.* Since $W_p \geq W_{p'}$ for $p \geq p'$ by Jensen's inequality [76, Remark 6.6], it suffices to lower bound W_1 . By Kantorovich duality [75, Theorem 1.14], we have that

$$W_1(\widehat{\mu}_n(m), \mu_n) \geq \int f d\widehat{\mu}_n(m) - \int f d\mu_n,$$

for any function $f : \Delta_{(d-1)} \rightarrow \mathbb{R}$ that is 1-Lipschitz with respect to $\text{dist}(\cdot, \cdot)$ on $\Delta_{(d-1)}$. We choose $f(X) = \frac{\|X\|_2^2}{2}$, and verify its Lipschitz property: for any $X, X' \in \Delta_{(d-1)}$ and $q \in [1, 2]$,

$$\begin{aligned}
|f(X') - f(X)| &= \frac{1}{2} \left| \|X'\|_2^2 - \|X\|_2^2 \right| \\
&= \frac{1}{2} (\|X'\|_2 + \|X\|_2) \left| \|X'\|_2 - \|X\|_2 \right| \\
&\leq \frac{1}{2} \cdot 2 \cdot \|X' - X\|_2 \leq \|X' - X\|_q.
\end{aligned}$$

Now, recall that $\mu_n = \frac{1}{n} \sum \delta_{X_i}$ and $\widehat{\mu}_n(m) = \frac{1}{n} \sum \delta_{\widehat{X}_i}$. Furthermore, recall $\mathbf{m} = (m_1, \dots, m_n)$ from (4.3) where we have assumed $\mathbf{u} = (\frac{1}{n}, \dots, \frac{1}{n})$. Such fixed \mathbf{u} also implies that \mathbf{m} and \mathbf{X} are independent. Putting these definitions together, we can write

$$\mathbb{E}W_1(\widehat{\mu}_n(m), \mu_n)$$

$$\begin{aligned}
&\geq \mathbb{E} \left[\int f d\hat{\mu}_n(m) - \int f d\mu_n \right] \\
&= \mathbb{E} \frac{1}{n} \sum_{i=1}^n \left(\frac{1}{2} \|\hat{X}_i\|_2^2 - \frac{1}{2} \|X_i\|_2^2 \right) \\
&= \frac{1}{n} \sum_{i=1}^n \frac{1}{2} \underbrace{\mathbb{E} \mathbb{1}_{\{m_i > 0\}} \left(\|\hat{X}_i\|_2^2 - \|X_i\|_2^2 \right)}_{(a)} + \frac{1}{n} \sum_{i=1}^n \frac{1}{2} \underbrace{\mathbb{E} \mathbb{1}_{\{m_i = 0\}} \left(\|\hat{X}_i\|_2^2 - \|X_i\|_2^2 \right)}_{(b)},
\end{aligned}$$

so that the problem simplifies to lower bounding the terms labeled (a) and (b).

We start with the simpler term (b). As stated in Section 1.1, \hat{X}_i may be chosen arbitrarily in $\Delta_{(d-1)}$ when $m_i = 0$, and hence, we use the trivial lower bound $\|\hat{X}_i\|_2^2 - \|X_i\|_2^2 \geq -1$. Using $m_i \sim \text{Binomial}(m, \frac{1}{n})$, this can be followed up with the estimate

$$\mathbb{E} \mathbb{1}_{\{m_i = 0\}} = \mathbb{P}(m_i = 0) = \left(1 - \frac{1}{n}\right)^m \leq \exp\left(-\frac{m}{n}\right)$$

to conclude that (b) $\geq -\exp\left(-\frac{m}{n}\right)$.

Next, we consider the term (a), rewriting it as

$$\mathbb{E} \mathbb{1}_{\{m_i > 0\}} \left(\|\hat{X}_i\|_2^2 - \|X_i\|_2^2 \right) = \mathbb{E} \left[\mathbb{1}_{\{m_i > 0\}} \mathbb{E} \left[\|\hat{X}_i\|_2^2 - \|X_i\|_2^2 \mid \mathbf{m}, \mathbf{X}, \mathbf{u} \right] \right].$$

Using the fact that

$$\hat{X}_i \mid \mathbf{m}, \mathbf{X}, \mathbf{u} \sim \frac{1}{m_i} \text{Multinomial}(X_i, m_i)$$

whenever $m_i > 0$, one can write the moments

$$\begin{aligned}
\mathbb{E} \left[\hat{X}_i \mid \mathbf{m}, \mathbf{X}, \mathbf{u} \right] &= X_i, \\
\text{tr} \left(\text{Cov} \left[\hat{X}_i \mid \mathbf{m}, \mathbf{X}, \mathbf{u} \right] \right) &= \frac{1 - \|X_i\|_2^2}{m_i},
\end{aligned}$$

so that

$$\mathbb{E} \left[\|\hat{X}_i\|_2^2 \mid \mathbf{m}, \mathbf{X}, \mathbf{u} \right] = \|X_i\|_2^2 + \frac{1}{m_i} (1 - \|X_i\|_2^2).$$

Hence, we simplify

$$\begin{aligned}
\mathbb{E} \left[\mathbb{1}_{\{m_i > 0\}} \mathbb{E} \left[\|\hat{X}_i\|_2^2 - \|X_i\|_2^2 \mid \mathbf{m}, \mathbf{X}, \mathbf{u} \right] \right] &= \mathbb{E} \left[\mathbb{1}_{\{m_i > 0\}} \frac{1}{m_i} (1 - \|X_i\|_2^2) \right] \\
&= \mathbb{E} \left[\mathbb{1}_{\{m_i > 0\}} \frac{1}{m_i} \right] (1 - \mathbb{E} \|X_i\|_2^2)
\end{aligned}$$

using the independence of \mathbf{m} and \mathbf{X} , and then lower bound

$$\mathbb{E} \left[\mathbb{1}_{\{m_i > 0\}} \frac{1}{m_i} \right] = \mathbb{E} \left[\frac{1}{m_i} \mid m_i > 0 \right] \mathbb{P}(m_i > 0) \geq \frac{1}{\mathbb{E}[m_i \mid m_i > 0]} \mathbb{P}(m_i > 0).$$

Finally, note that

$$\mathbb{E}[m_i \mid m_i > 0] = \frac{\mathbb{E} m_i}{\mathbb{P}(m_i > 0)} = \frac{m}{n} \frac{1}{\mathbb{P}(m_i > 0)},$$

and $\mathbb{P}(m_i > 0) = 1 - \mathbb{P}(m_i = 0) \geq 1 - \exp\left(-\frac{m}{n}\right)$, which concludes the calculation for (a).

Putting everything together,

$$\begin{aligned} \mathbb{E}W_1(\widehat{\mu}_n(m), \mu_n) &\geq \frac{1}{2} \left[\frac{n}{m} \left(1 - \exp\left(-\frac{m}{n}\right)\right)^2 (1 - \mathbb{E}\|X\|_2^2) - \exp\left(-\frac{m}{n}\right) \right] \\ &\geq \frac{1 - \mathbb{E}\|X\|_2^2}{4} \frac{n}{m}, \end{aligned}$$

provided $m \geq 2n \log \frac{4}{1 - \mathbb{E}\|X\|_2^2}$.

4.3. Proof of Theorem 2.6. The final goal is to obtain an optimal number of cells n given the m reads, which determines the number of reads per cell, in order to minimize $W_p(\widehat{\mu}_n(m), \mu)$ for $p \in [1, 2]$. We only focus on the optimal order of m in terms of n and ignore constants. Observe that a triangle inequality for W_p shows

$$W_p(\widehat{\mu}_n(m), \mu_n) + W_p(\mu_n, \mu).$$

Since $W_p(\widehat{\mu}_n(m), \mu_n)$ is controlled by Theorem 2.4, let's pay attention to $W_p(\mu_n, \mu)$.

There have been many papers studying to deduce the tight rate of the convergence of empirical distributions and concentration inequalities of W_p for $p \geq 1$. Regarding the state-of-art results in this area, we refer readers to [6–8, 18, 24, 33, 43, 51, 53, 54] and references therein. In the present paper we adopt [53] since $\Delta_{(d-1)}$ is bounded.

LEMMA 4.9. [53, Theorem 1, Proposition 20] *Let μ have support with diameter D , and let $d_p^*(\mu)$ be the upper Wasserstein dimension. Let $1 \leq p < \infty$. If $k > \max\{d_p^*(\mu), 2p\}$, then*

$$(4.10) \quad \mathbb{E}[W_p(\mu, \mu_n)] \leq C_1 n^{-\frac{1}{k}} + C_2 n^{-\frac{1}{2p}} = O\left(n^{-\frac{1}{k}}\right)$$

for some C_1 and C_2 which are given as

$$C_1 = 3^{\frac{3k}{k-2p} + \frac{1}{p}} \left(\frac{1}{3^{\frac{k}{2}-p} - 1} + 3 \right)^{\frac{1}{p}}, \quad C_2 = \left(\frac{27}{\varepsilon'} \right)^{\frac{k}{2p}}$$

where $\varepsilon' > 0$ is a constant which satisfies $d(\varepsilon, \varepsilon^{\frac{sp}{s-2p}}; \mu) \leq k$ for all $\varepsilon \leq \varepsilon'$.

Furthermore, for any $t > 0$,

$$(4.11) \quad \mathbb{P}\left(W_p^p(\mu, \mu_n) \geq t + \mathbb{E}[W_p^p(\mu, \mu_n)]\right) \leq \exp\left(-\frac{2nt^2}{D^{2p}}\right).$$

REMARK 4.10. As mentioned in Theorem 2.2, such k is the intrinsic dimension of μ , or the dimension of its support.

Note that in equation (4.10), the second term (involving C_2) is small compared to the first term since $k > 2p$. Therefore, while C_2 may depend on μ (through ε'), the leading term does not depend on the dimension.

There is an alternative upper bound in [53][Proposition 10] to get rid of C_2 . Let $d_{\geq \varepsilon}(\tau; \mu) := \sup_{\varepsilon' \in [\varepsilon, \frac{1}{9}]} d(\varepsilon, \tau; \mu)$, and $k_n := \inf_{\varepsilon > 0} \max\left\{d_{\geq \varepsilon}(\varepsilon^p; \mu), \frac{\log n}{-\log \varepsilon}\right\}$. If $k_n > 2p$, then

$$\mathbb{E}[W_p(\mu, \mu_n)] \leq C_1 n^{-\frac{1}{k_n}}$$

where C_1 depends on p and k_n . However the choice of k_n is harder to interpret than $d_p^*(\mu)$. Also, it seems to depend on μ itself.

PROOF OF THEOREM 2.6. Fix $\alpha \in (0, 1)$ and $p \in [1, 2]$. Assume that there is some $k > 0$ such that $k > \max\{d_p^*(\mu), 2p\}$. Since $\text{diam}(\Delta_{(d-1)}) \leq 2$, by (4.11), $W_p(\mu_n, \mu) \leq \mathbb{E}W_p(\mu_n, \mu) + n^{-q}$ with probability $1 - \exp\left(-\frac{1}{2^{2p-1}}n^{1-2q}\right)$ for any $0 < q < \frac{1}{2}$. Let $q = \frac{1}{4}$ for simplicity. Then, with probability $1 - \exp\left(-\frac{\sqrt{n}}{2^{2p-1}}\right)$

$$W_p(\mu_n, \mu) \leq O(n^{-\frac{1}{k}}).$$

Let $\epsilon = n^{-t}$ for some $t > 0$. Given m , let n satisfy (2.4). Ignoring the lower order term, a maximum such n should satisfy

$$(4.12) \quad n \geq \left(\frac{c_* m}{8(1+\alpha)\mathbb{E}\|X\|_0} \right)^{\frac{1}{1+2t}}.$$

Combining (2.5) with (4.11), a triangle inequality implies

$$W_p(\hat{\mu}_n(m), \mu) \leq O(n^{-t}) + O(n^{-\frac{1}{k}})$$

with probability $1 - O(n^{-\frac{\alpha}{2}}) = (1 - O(n^{-\frac{\alpha}{2}})) \left(1 - \exp\left(-\frac{\sqrt{n}}{2^{2p-1}}\right)\right)$. Let's optimize $O(n^{-t}) + O(n^{-\frac{1}{k}})$ by choosing t . Let $n(t)$ satisfy (4.12) given m and t . Then,

$$O(n(t)^{-t}) + O(n(t)^{-\frac{1}{k}}) = O\left(e^{-t \log n(t)}\right) + O\left(e^{-\frac{1}{k} \log n(t)}\right) = O\left(e^{-\min\{t, \frac{1}{k}\} \log n(t)}\right).$$

If $t > \frac{1}{k}$, the order is $O\left(n(t)^{-\frac{1}{k}}\right)$. Notice that $n(t)$ is decreasing with respect to t : it is trivial due to (4.12). Hence, $n(t)^{-\frac{1}{k}}$ decreases as t decreases until $t = \frac{1}{k}$. If $t < \frac{1}{k}$, the order is

$$O\left(n(t)^{-t}\right) = O\left(e^{-t \log n(t)}\right) = O\left(\exp\left(-\frac{t(\log(c_* m) - \log(8(1+\alpha)\mathbb{E}\|X\|_0))}{1+2t}\right)\right).$$

It is easy to check that

$$\begin{aligned} & \partial_t \left(\frac{t(\log(c_* m) - \log(8(1+\alpha)\mathbb{E}\|X\|_0))}{1+2t} \right) \\ &= \frac{(\log(c_* m) - \log(8(1+\alpha)\mathbb{E}\|X\|_0)) - 2t(\log(c_* m) - \log(8(1+\alpha)\mathbb{E}\|X\|_0))}{(1+2t)^2} \\ &\geq 0 \end{aligned}$$

provided that $\log(c_* m) \geq \log(8(1+\alpha)\mathbb{E}\|X\|_0)$ and $t \leq \frac{1}{2}$. Let $m_0(c_*, \alpha, \mathbb{E}\|X\|_0)$ be a positive constant satisfying $\log(c_* m) > \log(8(1+\alpha)\mathbb{E}\|X\|_0)$. Since $m \geq m_0$ and $k > 4$, increasing t up to $\frac{1}{k}$ decreases $O\left(n(t)^{-t}\right)$. Combining the case for $t > \frac{1}{k}$, we can conclude that the optimal $t = \frac{1}{k}$. \square

5. Conclusion and future works. In this paper we analyze the distance between an empirical distribution of cells, sampled with scRNA-seq, and the true population. When the total number of reads is fixed, sampling more cells does not always make the empirical distribution $\hat{\mu}$ closer to the true distribution μ . In order to minimize the Wasserstein distance between $\hat{\mu}$ and μ , the number of cells n should scale with the number of reads m like

$$n \sim m^{\frac{k}{k+2}},$$

where k is the intrinsic dimension of the true distribution.

In future work, it would be interesting to analyze optimal sequencing depth for different estimation problems. Fewer reads per cell may be optimal for structured estimation problems

such as clustering or shape-constrained density estimation. And adding additional dimensions such as space or time would present interesting analytical opportunities for spatial transcriptomics or trajectory inference. Our results for general empirical distributions should provide a good starting point to analyze these diverse contexts and extract as much information as possible from a limited sequencing budget.

We note that it would be feasible to explore different mathematical models for noisy empirical distributions, the beyond normalized multinomial sampling of reads for scRNA-seq. Indeed, most data are observed with measurement noise, and multinomial sampling plays no crucial role in our analysis: the concentration inequality, (4.2), is the only property used in the proof. We hope that our work serves as a starting point for investigating noisy empirical distributions in general settings.

Finally, one could ask the same question under high-dimensional setting. In our model, the ambient and intrinsic dimensions d and k are fixed, and only n and m grow. In various high-dimensional statistics, however, d also grows as n does (also k sometimes grows but slower than d). What happens d also grows? In this case, $\frac{m}{n} \rightarrow \alpha$ and $\frac{d}{n} \rightarrow \beta$. Under this setting, can the Wasserstein distance between $\hat{\mu}_n(m)$ and μ vanish? Is there any phase transition of the Wasserstein distance in terms of α and β ? We believe it is a new type of high-dimensional problem of interest both theoretically and practically.

Acknowledgments. The majority of the work for this publication was done when JK was at University of British Columbia and PIMS. JK appreciates their supports and hospitality.

Funding. JK thanks to PIMS postdoctoral fellowship through the Kantorovich Initiative PIMS Research Network (PRN) as well as National Science Foundation grant NSF-DMS 2133244. GS and SK are supported by a CIHR PG and an NSERC DG. We thank PIMS for their generous support; report identifier PIMS-20240912-PRN01.

APPENDIX A: RESULTS ON ADDITIONAL DATASETS

We validate our theoretical results on two other scRNA-seq datasets – the *sea urchin* dataset [47] and the *Arabidopsis* dataset [66]. Further details about the specific data files and preprocessing steps are available in Section B.1.

As discussed in Section 3.1, the datasets contain cells-by-genes counts matrices \mathbf{C} of (UMI) reads recorded in sequencing experiments. The corresponding population distributions μ are constructed as per (3.1), with statistics

- $d = 1000$, $N = 5580$, $k = 10.092$, and $\mathbb{E}_{P \sim \mu} \|X\|_0 \simeq 113$ for the sea urchin dataset,
- $d = 1000$, $N = 5801$, $k = 7.432$ and $\mathbb{E}_{P \sim \mu} \|X\|_0 \simeq 90$ for the *Arabidopsis* dataset.

Here, the intrinsic dimensions k are approximated via the heuristic from Section 3.1.3; see Section B.2 and Figure 7. We repeat the experiment from Section 3.2 on the two datasets below; in particular, we assume uniform cell weights.

As in Section 3.2, for various pairs of n and m , we simulate the noisy empirical distribution $\hat{\mu}_n(m)$ for ten (10) independent trials, and compute the mean Wasserstein error $W_1(\hat{\mu}_n(m), \mu)$ over those trials. Contours of mean $W_1(\hat{\mu}_n(m), \mu)$ over m - n axes, for both datasets, are plotted in Figure 6. For each budget m tested, we identify the number of cells $n = n^*$ that yields the lowest mean $W_1(\hat{\mu}_n(m), \mu)$. These m - n^* relationships, also shown in Figure 6, appear to be well captured by our theoretically derived optimal allocation

$$n \sim \left(\frac{Cm}{\mathbb{E}\|X\|_0} \right)^{1 - \frac{2}{2+k}}$$

where C is a $\Theta(1)$ constant. In the plots, we used $C = 1$ for the sea urchin dataset, and $C = 6$ for the *Arabidopsis* dataset.

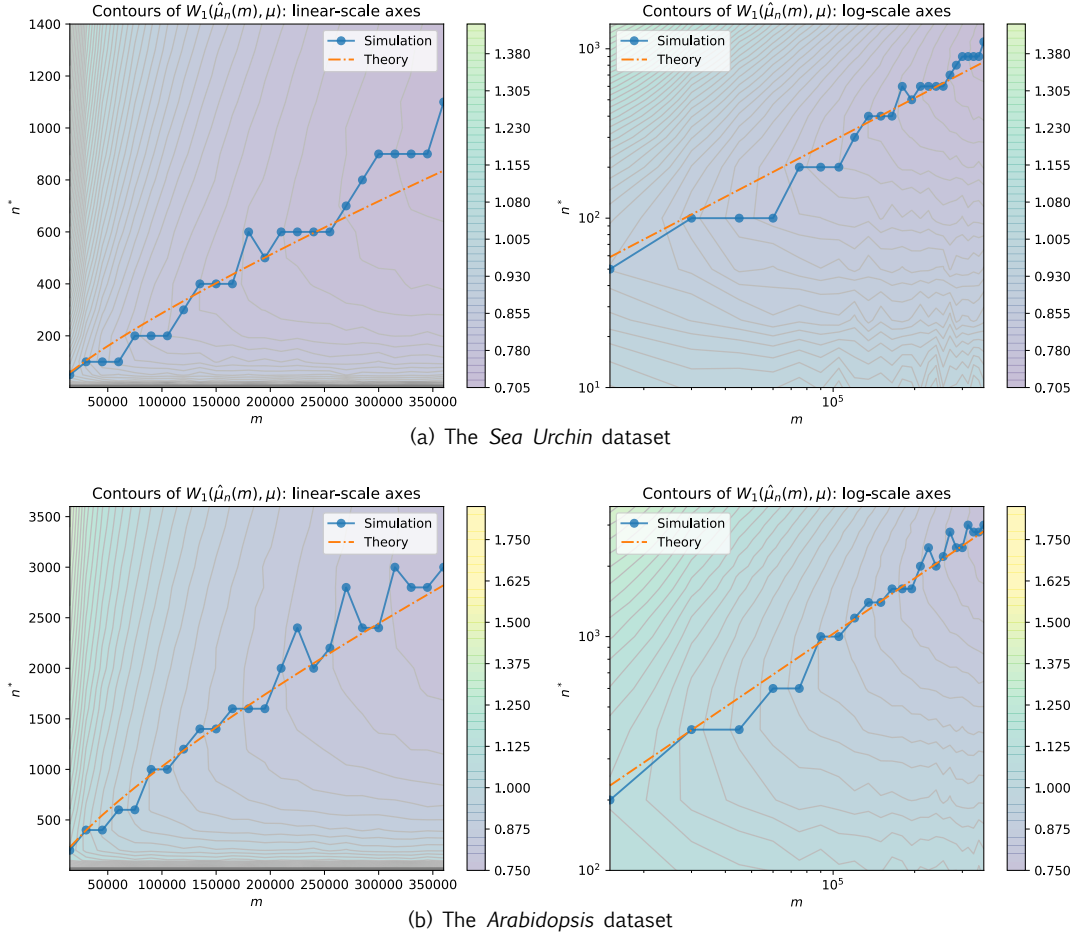


FIGURE 6. **Optimal allocation (m - n relationship) with uniform cell weights for (a) the sea urchin dataset, and (b) the Arabidopsis dataset.** For each dataset, the contours and the colour scales show $W_1(\hat{\mu}_n(m), \mu)$ averaged over ten (10) independent realizations of $\hat{\mu}_n(m)$, for various pairs of m and n on a grid. The m and n axes are plotted in a linear scale on the left panels, and in a log scale on the right panels. The optimal values of n^* for each m , as observed in these simulations, are plotted with blue solid dots. Our theoretically derived optimal allocations are plotted as orange dash-dot lines.

APPENDIX B: EXPERIMENT DETAILS

In this section, we provide further details on the dataset, preprocessing steps, and software packages used in the experiments presented in Section 3.

B.1. Datasets and preprocessing. Data processing is done in python, using the packages Scanpy [81] and Anndata [77]. Below, we describe details and preprocessing steps specific to the three datasets studied. The resulting preprocessed counts matrices \mathbf{C} are then used as described in Section 3.

The cellular reprogramming dataset. This dataset is published in Schiebinger et al. [65], and is publicly available through the NCBI Gene Expression Omnibus with identification number GSE122662. We use the counts matrices from the files `GSM3195748_D15.5_serum_C1_gene_bc_mat.h5` and `GSM3195749_D15.5_serum_C2_gene_bc_mat.h5`. Scanpy's function `read_10x_h5` is used to read in the data files, and the resulting

Anndata objects are concatenated via an inner join. The result is a (annotated) cells-by-genes counts matrix of unique molecular identifier (UMI) reads.

We preprocess this data by first filtering out genes that are expressed in fewer than 10 cells, and then subsetting to the top $d = 1000$ highly variable genes (as determined by Scanpy’s `highly_variable_genes` function with `flavor = "seurat_v3"`). Note that we do **not** use any nonlinear transformation on the data, such as the standard `log1p` transform.

The sea urchin dataset. This dataset is affiliated with Massri et al. [47]. The particular data file we used is made available on <https://personal.math.ubc.ca/~sharvaj/> as `adata_raw_0715_SCT.h5ad`, whose data matrix consists of counts post an `sctransform` [27] followed by a `log1p` transform. Scanpy’s function `read_h5ad` is used to read in the data, and the resulting Anndata object is subsampled to 6000 cells at random (using `scanpy.pp.subsample`) to reduce the computational cost. Next the entries of data matrix (`AnnData.X`) are transformed as $t \mapsto \exp(t) - 1$ in order to reverse the `log1p` transform and obtain a cells-by-genes matrix of integer counts.

We preprocess this matrix by filtering out cells with fewer than 2000 counts, and then filtering out genes that are expressed in fewer than 10 cells. Finally, we subset to the top $d = 1000$ highly variable genes (as determined by Scanpy’s `highly_variable_genes` function with `flavor = "seurat_v3"`).

The Arabidopsis dataset. The particular data file we used is made available on <https://personal.math.ubc.ca/~sharvaj/> as `recovery_counts.h5ad`, which contains a cells-by-genes matrix of integer counts. Scanpy’s function `read_h5ad` is used to read in the data, and the resulting Anndata object is subsampled to 6000 cells at random (using `scanpy.pp.subsample`) to reduce the computational cost.

As before, we filter out cells with fewer than 2000 counts, and then filter out genes that are expressed in fewer than 10 cells. Finally, we subset to the top $d = 1000$ highly variable genes (as determined by Scanpy’s `highly_variable_genes` function with `flavor = "seurat_v3"`).

B.2. Estimating intrinsic dimensions. Recall that μ is constructed as

$$(B.1) \quad \mu = \frac{1}{N} \sum_{\ell=1}^N \delta_{C_\ell / \|C_\ell\|_1}$$

where C_ℓ is the ℓ -th row of the (preprocessed) counts matrix \mathbf{C} . As we keep only the top 1000 highly variable genes, the ambient dimension is $d = 1000$ for all the datasets considered.

We employ the heuristic discussed in Section 3.1.3 to estimate the intrinsic dimension k of μ . In particular, for various values of n , we repeatedly draw i.i.d. samples from μ to form n -sample (true) empirical distributions μ_n , and compute $W_1(\mu, \mu_n)$ for each such trial. Then, we fit a straight line to the resulting set of pairs $(\log n, \log W_1(\mu, \mu_n))$, the slope of which approximates $-1/k$. As seen in Figure 7, this procedure gives $k = 9.718$ for the reprogramming dataset, $k = 10.092$ for the sea urchin dataset, and $k = 7.432$ for the Arabidopsis dataset.

B.3. Constructing lower-dimensional distributions μ_k . Recall the lower-dimensional synthetic distributions μ_k from Section 3.3. Here, we describe our procedure for constructing those distributions from the reprogramming dataset.

The support of μ as defined in (B.1) is a finite set of vectors in the simplex; it can be packaged as a matrix $M \in \mathbb{R}_+^{N \times d}$ whose rows are the atoms of μ . Now, consider a rank- r non-negative matrix factorization $M \simeq WH$, where $W \in \mathbb{R}_+^{N \times r}$ and $H \in \mathbb{R}_+^{r \times d}$. The rank

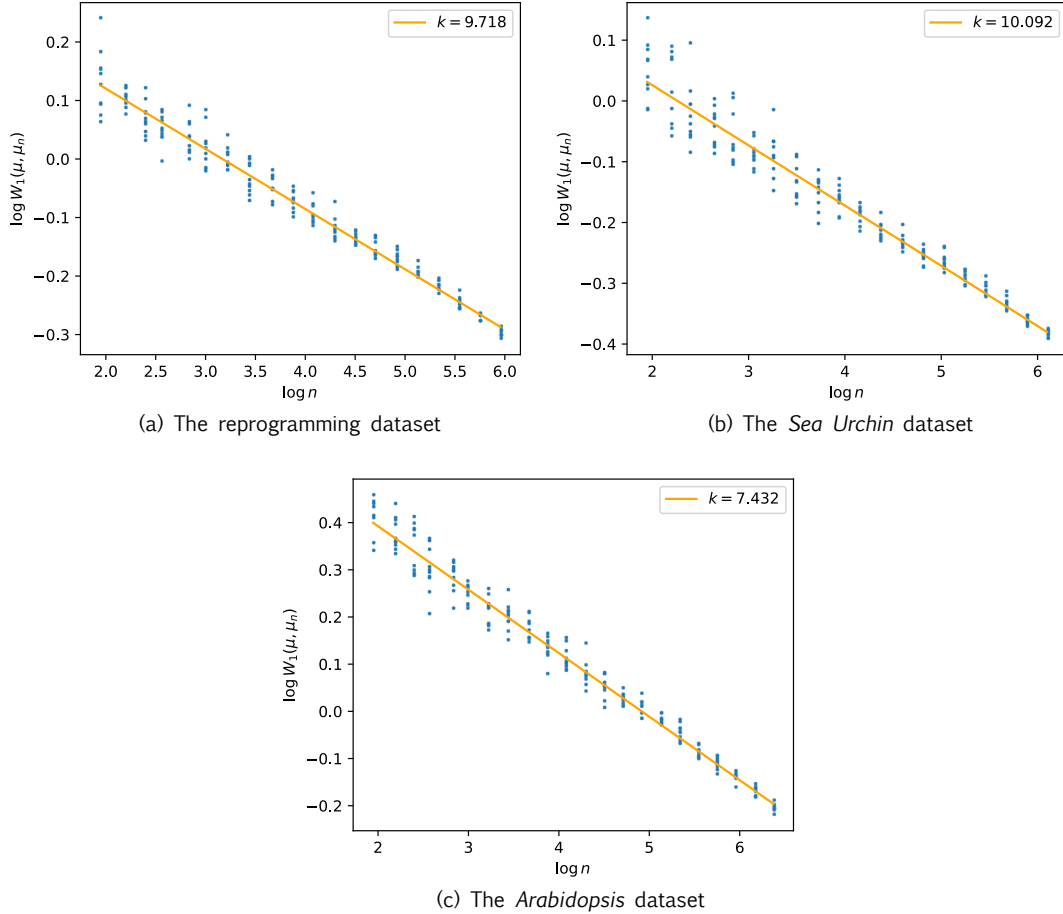


FIGURE 7. Estimating the intrinsic dimension k of μ constructed from (a) the reprogramming dataset, (b) the sea urchin dataset, and (c) the *Arabidopsis* dataset. As per the heuristic from Section 3.1.3, we fit a straight line to the $\log n$ - $\log W_1(\mu, \mu_n)$ relationship, the slope of which approximates $-1/k$.

of $M_r := WH$ is at most r , and we can rescale the rows of M_r to the simplex without changing the rank. The result is a set of vectors in the simplex that is also contained in an r -dimensional linear subspace. Hence, the rows of this rescaled version of M_r form the support of our at-most r -dimensional synthetic distribution. We compute its intrinsic dimension k via the heuristic from Section 3.1.3 again, noting that $k \leq r$ necessarily; see Figure 8. Some statistics are reported in Table 1.

B.4. Computing optimal transport. The experiments of Section 3 involve computing Wasserstein distances between finitely supported atomic measures. The Python Optimal Transport package [23] provides various tools for this. We used the function `emd2`, which involves no additional regularization, together with the `cityblock` distance.

REFERENCES

- [1] AHLMANN-ELTZE, C. and HUBER, W. (2023). Comparison of transformations for single-cell RNA-seq data. *Nature Methods* **20** 665–672.
- [2] BACHER, R. and KENDZIORSKI, C. (2016). Design and computational analysis of single-cell RNA-sequencing experiments. *Genome biology* **17** 1–14.

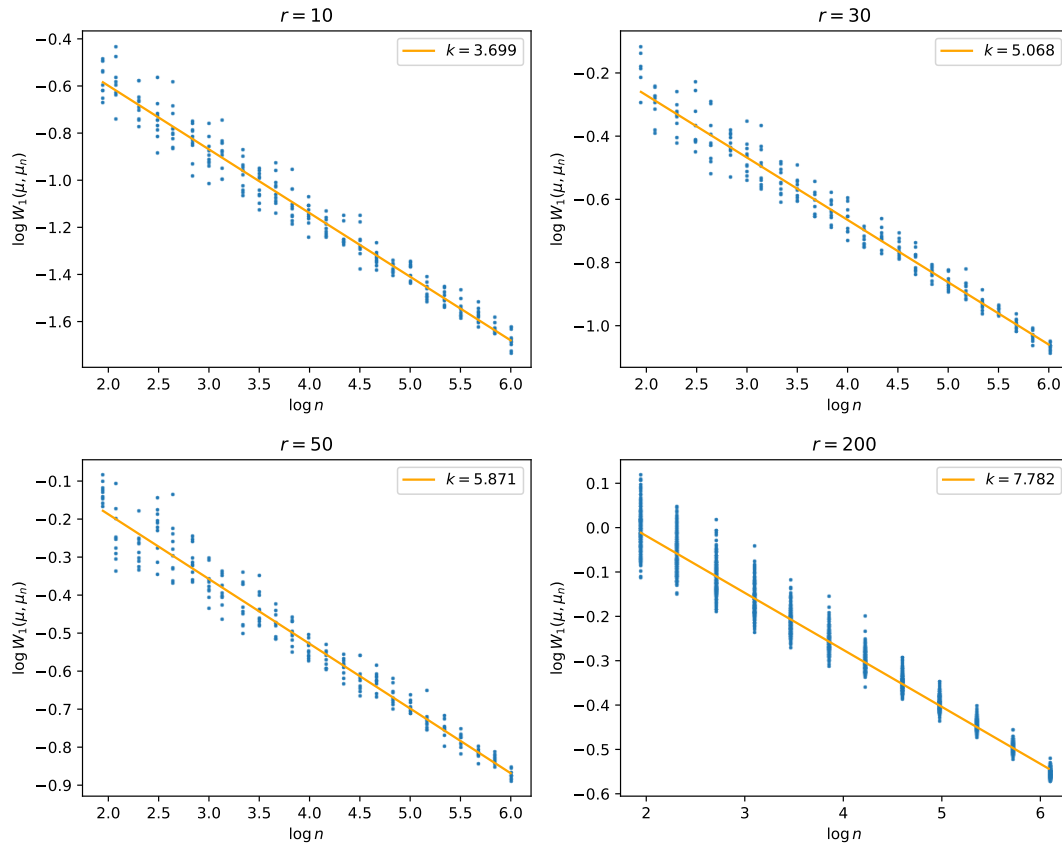


FIGURE 8. *Estimating the intrinsic dimensions k of the synthetic distributions μ_k constructed as in Section B.3. The rank r is the one used for matrix factorization. As per the heuristic from Section 3.1.3, we fit a straight line to the $\log n$ - $\log W_1(\mu, \mu_n)$ relationship, the slope of which approximates $-1/k$.*

Rank r	Relative error	Intrinsic dimension k	Average sparsity $\mathbb{E}_{X \sim \mu_k} \ X\ _0$
10	0.45	3.699	987
30	0.30	5.068	976
50	0.24	5.871	981
200	0.12	7.782	984

TABLE 1

Statistics of the synthetic distributions μ_k . The rank r is the one used for matrix factorization, and the relative error of the factorization is defined as $\|\bar{M}_r - M\|_F / \|M\|_F$ where \bar{M}_r is the rescaled version of WH . The intrinsic dimension k is computed via the heuristic from Section 3.1.3. Finally, recall that $d = 1000$ is the upper bound on the average sparsities.

- [3] BEIGLBÖCK, M. and JUILLET, N. (2016). On a problem of optimal transport under marginal martingale constraints. *Ann. Probab.* **44** 42–106. <https://doi.org/10.1214/14-AOP966> MR3456332
- [4] BENAMOU, J.-D. and BRENIER, Y. (2000). A computational fluid mechanics solution to the Monge-Kantorovich mass transfer problem. *Numer. Math.* **84** 375–393. <https://doi.org/10.1007/s002110050002> MR1738163
- [5] BLOCK, A., JIA, Z., POLYANSKIY, Y. and RAKHLIN, A. (2022). Intrinsic Dimension Estimation Using Wasserstein Distance. *Journal of Machine Learning Research* **23** 1–37.

- [6] BOISSARD, E. (2011). Simple bounds for convergence of empirical and occupation measures in 1-Wasserstein distance. *Electron. J. Probab.* **16** no. 83, 2296–2333. <https://doi.org/10.1214/EJP.v16-958> MR2861675
- [7] BOISSARD, E. and LE GOUIC, T. (2014). On the mean speed of convergence of empirical and occupation measures in Wasserstein distance. *Ann. Inst. Henri Poincaré Probab. Stat.* **50** 539–563. <https://doi.org/10.1214/12-AIHP517> MR3189084
- [8] BOLLEY, F., GUILLIN, A. and VILLANI, C. (2007). Quantitative concentration inequalities for empirical measures on non-compact spaces. *Probab. Theory Related Fields* **137** 541–593. <https://doi.org/10.1007/s00440-006-0004-7> MR2280433
- [9] BRENIER, Y. (1991). Polar factorization and monotone rearrangement of vector-valued functions. *Comm. Pure Appl. Math.* **44** 375–417. <https://doi.org/10.1002/cpa.3160440402> MR1100809
- [10] CAFFARELLI, L. A. (2000). Monotonicity properties of optimal transportation and the FKG and related inequalities. *Comm. Math. Phys.* **214** 547–563. <https://doi.org/10.1007/s002200000257> MR1800860
- [11] CAFFARELLI, L. and FIGALLI, A. (2013). Regularity of solutions to the parabolic fractional obstacle problem. *J. Reine Angew. Math.* **680** 191–233. <https://doi.org/10.1515/crelle.2012.036> MR3100955
- [12] CARRILLO, J. A., DIFRANCESCO, M., FIGALLI, A., LAURENT, T. and SLEP'CEV, D. (2011). Global-in-time weak measure solutions and finite-time aggregation for nonlocal interaction equations. *Duke Math. J.* **156** 229–271. <https://doi.org/10.1215/00127094-2010-211> MR2769217
- [13] CHIZAT, L. and BACH, F. (2018). On the global convergence of gradient descent for over-parameterized models using optimal transport. *Advances in neural information processing systems* **31**.
- [14] CUTURI, M. (2013). Sinkhorn Distances: Lightspeed Computation of Optimal Transport. In *Advances in Neural Information Processing Systems* (C. J. BURGESS, L. BOTTOU, M. WELLING, Z. GHAHRAMANI and K. Q. WEINBERGER, eds.) **26**. Curran Associates, Inc.
- [15] DAL MOLIN, A. and DI CAMILLO, B. (2019). How to design a single-cell RNA-sequencing experiment: pitfalls, challenges and perspectives. *Briefings in bioinformatics* **20** 1384–1394.
- [16] DE BORTOLI, V., THORNTON, J., HENG, J. and DOUCET, A. (2021). Diffusion schrödinger bridge with applications to score-based generative modeling. *Advances in Neural Information Processing Systems* **34** 17695–17709.
- [17] DIAO, M. Z., BALASUBRAMANIAN, K., CHEWI, S. and SALIM, A. (2023). Forward-backward Gaussian variational inference via JKO in the Bures-Wasserstein space. In *International Conference on Machine Learning* 7960–7991. PMLR.
- [18] DUDLEY, R. M. (1969). The Speed of Mean Glivenko-Cantelli Convergence. *The Annals of Mathematical Statistics* **40** 40–50.
- [19] ECKER, J. R., GESCHWIND, D. H., KRIEGSTEIN, A. R., NGAI, J., OSTEN, P., POLIOUDAKIS, D., REGEV, A., SESTAN, N., WICKERSHAM, I. R. and ZENG, H. (2017). The BRAIN initiative cell census consortium: lessons learned toward generating a comprehensive brain cell atlas. *Neuron* **96** 542–557.
- [20] EFRON, B. (2016). Empirical Bayes deconvolution estimates. *Biometrika* **103** 1–20.
- [21] FIGALLI, A., MAGGI, F. and PRATELLI, A. (2010). A mass transportation approach to quantitative isoperimetric inequalities. *Invent. Math.* **182** 167–211. <https://doi.org/10.1007/s00222-010-0261-z> MR2672283
- [22] FIGALLI, A., FUSCO, N., MAGGI, F., MILLOT, V. and MORINI, M. (2015). Isoperimetry and stability properties of balls with respect to nonlocal energies. *Comm. Math. Phys.* **336** 441–507. <https://doi.org/10.1007/s00220-014-2244-1> MR3322379
- [23] FLAMARY, R., COURTY, N., GRAMFORT, A., ALAYA, M. Z., BOISBUNON, A., CHAMBON, S., CHAPEL, L., CORENFLOS, A., FATRAS, K., FOURNIER, N., GAUTHERON, L., GAYRAUD, N. T. H., JANATI, H., RAKOTOMAMONJY, A., REDKO, I., ROLET, A., SCHUTZ, A., SEGUY, V., SUTHERLAND, D. J., TAVENARD, R., TONG, A. and VAYER, T. (2021). POT: Python Optimal Transport. *Journal of Machine Learning Research* **22** 1–8.
- [24] FOURNIER, N. and GUILLIN, A. (2015). On the rate of convergence in Wasserstein distance of the empirical measure. *Probab. Theory Related Fields* **162** 707–738. <https://doi.org/10.1007/s00440-014-0583-7> MR3383341
- [25] GOZLAN, N., ROBERTO, C., SAMSON, P.-M. and TETALI, P. (2017). Kantorovich duality for general transport costs and applications. *Journal of Functional Analysis* **273** 3327–3405. <https://doi.org/10.1016/j.jfa.2017.08.015>
- [26] GRABSKI, I. N., STREET, K. and IRIZARRY, R. A. (2023). Significance analysis for clustering with single-cell RNA-sequencing data. *Nature Methods* **20** 1196–1202.
- [27] HAFEMEISTER, C. and SATIJA, R. (2019). Normalization and variance stabilization of single-cell RNA-seq data using regularized negative binomial regression. *Genome biology* **20** 296.

- [28] HAMDUCHE, M., HENRY-LABORDERE, P. and PHAM, H. (2023). Generative modeling for time series via Schrödinger bridge. *arXiv preprint arXiv:2304.05093*.
- [29] HAQUE, A., ENGEL, J., TEICHMANN, S. A. and LÖNNBERG, T. (2017). A practical guide to single-cell RNA-sequencing for biomedical research and clinical applications. *Genome medicine* **9** 1–12.
- [30] HEIMBERG, G., BHATNAGAR, R., EL-SAMAD, H. and THOMSON, M. (2016). Low dimensionality in gene expression data enables the accurate extraction of transcriptional programs from shallow sequencing. *Cell systems* **2** 239–250.
- [31] HOBSON, D. and NEUBERGER, A. (2012). Robust bounds for forward start options. *Mathematical Finance: An International Journal of Mathematics, Statistics and Financial Economics* **22** 31–56.
- [32] HUANG, M., WANG, J., TORRE, E., DUECK, H., SHAFFER, S., BONASIO, R., MURRAY, J. I., RAJ, A., LI, M. and ZHANG, N. R. (2018). SAVER: gene expression recovery for single-cell RNA sequencing. *Nature methods* **15** 539–542.
- [33] HÜTTER, J.-C. and RIGOLLET, P. (2021). Minimax estimation of smooth optimal transport maps. *Ann. Statist.* **49** 1166–1194. <https://doi.org/10.1214/20-aos1997> MR4255123
- [34] JAITIN, D. A., KENIGSBERG, E., KEREN-SHAUL, H., ELEFANT, N., PAUL, F., ZARETSKY, I., MILDNER, A., COHEN, N., JUNG, S., TANAY, A. et al. (2014). Massively parallel single-cell RNA-seq for marker-free decomposition of tissues into cell types. *Science* **343** 776–779.
- [35] KANTOROVICH, L. V. (1942). On the translocation of masses. In *Dokl. Akad. Nauk. USSR (NS)* **37** 199–201.
- [36] KANTOROVICH, L. V. (1948). On a problem of Monge. In *CR (Doklady) Acad. Sci. URSS (NS)* **3** 225–226.
- [37] KIM, Y.-H. and MCCANN, R. J. (2010). Continuity, curvature, and the general covariance of optimal transportation. *J. Eur. Math. Soc. (JEMS)* **12** 1009–1040. <https://doi.org/10.4171/JEMS/221> MR2654086
- [38] KIM, J., KIM, Y.-H., RUAN, Y. and WARREN, A. (2024). Statistical inference of convex order by Wasserstein projection.
- [39] KIVIOJA, T., VÄHÄRAUTIO, A., KARLSSON, K., BONKE, M., ENGE, M., LINNARSSON, S. and TAIPALE, J. (2012). Counting absolute numbers of molecules using unique molecular identifiers. *Nature methods* **9** 72–74.
- [40] KLEIN, A., MAZUTIS, L., AKARTUNA, I., TALLAPRAGADA, N., VERES, A., LI, V., PESHKIN, L., WEITZ, D. and KIRSCHNER, M. (2015). Droplet Barcoding for Single-Cell Transcriptomics Applied to Embryonic Stem Cells. *Cell* **161** 1187–1201. <https://doi.org/10.1016/j.cell.2015.04.044>
- [41] LAMBERT, M., CHEWI, S., BACH, F., BONNABEL, S. and RIGOLLET, P. (2022). Variational inference via Wasserstein gradient flows. *Advances in Neural Information Processing Systems* **35** 14434–14447.
- [42] LAVENANT, H., ZHANG, S., KIM, Y.-H., SCHIEBINGER, G. et al. (2024). Toward a mathematical theory of trajectory inference. *The Annals of Applied Probability* **34** 428–500.
- [43] LEDOUX, M. and ZHU, J.-X. (2021). On optimal matching of Gaussian samples III. *Probab. Math. Statist.* **41** 237–265. <https://doi.org/10.37190/0208-4147.41.2.3> MR4359822
- [44] LOTT, J. and VILLANI, C. (2004). Ricci curvature for metric-measure spaces via optimal transport. *Annals of Mathematics* **169** 903–991.
- [45] MACOSKO, E. Z., BASU, A., SATIJA, R., NEMESH, J., SHEKHAR, K., GOLDMAN, M., TIROSH, I., BIALAS, A. R., KAMITAKI, N., MARTERSTECK, E. M. et al. (2015). Highly parallel genome-wide expression profiling of individual cells using nanoliter droplets. *Cell* **161** 1202–1214.
- [46] MASOERO, L., CAMERLENGHI, F., FAVARO, S. and BRODERICK, T. (2021). More for less: predicting and maximizing genomic variant discovery via Bayesian nonparametrics. *Biometrika* **109** 17–32. <https://doi.org/10.1093/biomet/asab012>
- [47] MASSRI, A. J., BERRIO, A., AFANASSIEV, A., GREENSTREET, L., PIPHO, K., BYRNE, M., SCHIEBINGER, G., MCCLAY, D. R. and WRAY, G. A. (2025). Single-Cell Transcriptomics Reveals Evolutionary Reconfiguration of Embryonic Cell Fate Specification in the Sea Urchin *Heliocidaris erythrogramma*. *Genome Biology and Evolution* **17** evae258. <https://doi.org/10.1093/gbe/evae258>
- [48] MCCANN, R. J. (1994). *A convexity theory for interacting gases and equilibrium crystals*. Princeton University.
- [49] MCCANN, R. J. (1997). A convexity principle for interacting gases. *Adv. Math.* **128** 153–179. <https://doi.org/10.1006/aima.1997.1634> MR1451422
- [50] MEI, S., MONTANARI, A. and NGUYEN, P.-M. (2018). A mean field view of the landscape of two-layer neural networks. *Proceedings of the National Academy of Sciences* **115** E7665–E7671.
- [51] MÉRIGOT, Q., SANTAMBROGIO, F. and SARRAZIN, C. (2021). Non-asymptotic convergence bounds for Wasserstein approximation using point clouds. *Advances in Neural Information Processing Systems* **34** 12810–12821.
- [52] MONGE, G. (1781). Mémoire sur la théorie des déblais et des remblais. *Mem. Math. Phys. Acad. Royale Sci.* 666–704.

- [53] NILES-WEED, J. and BACH, F. (2019). Sharp asymptotic and finite-sample rates of convergence of empirical measures in Wasserstein distance. *Bernoulli* **25** 2620–2648. <https://doi.org/10.3150/18-BEJ1065> MR4003560
- [54] NILES-WEED, J. and BERTHET, Q. (2022). Minimax estimation of smooth densities in Wasserstein distance. *Ann. Statist.* **50** 1519–1540. <https://doi.org/10.1214/21-aos2161> MR4441130
- [55] OTTO, F. (2001). The geometry of dissipative evolution equations: the porous medium equation. *Comm. Partial Differential Equations* **26** 101–174.
- [56] OTTO, F. and VILLANI, C. (2000). Generalization of an Inequality by Talagrand and Links with the Logarithmic Sobolev Inequality. *Journal of Functional Analysis* **173** 361–400.
- [57] PEYRÉ, G. and CUTURI, M. (2019). Computational Optimal Transport: With Applications to Data Science. *Foundations and trends in machine learning* **11** 355–607.
- [58] POLLEN, A. A., NOWAKOWSKI, T. J., SHUGA, J., WANG, X., LEYRAT, A. A., LUI, J. H., LI, N., SZPANKOWSKI, L., FOWLER, B., CHEN, P. et al. (2014). Low-coverage single-cell mRNA sequencing reveals cellular heterogeneity and activated signaling pathways in developing cerebral cortex. *Nature biotechnology* **32** 1053–1058.
- [59] PYDI, M. S. and JOG, V. (2021). The Many Faces of Adversarial Risk. In *Thirty-Fifth Conference on Neural Information Processing Systems*.
- [60] QIAN, J., FRUIT, R., PIROTTA, M. and LAZARIC, A. (2020). Concentration inequalities for multinoulli random variables. *arXiv preprint arXiv:2001.11595*.
- [61] QIU, C., CAO, J., MARTIN, B. K., LI, T., WELSH, I. C., SRIVATSAN, S., HUANG, X., CALDERON, D., NOBLE, W. S., DISTECHE, C. M. et al. (2022). Systematic reconstruction of cellular trajectories across mouse embryogenesis. *Nature genetics* **54** 328–341.
- [62] ROCH, S. (2024). *Modern discrete probability: An essential toolkit*. Cambridge University Press.
- [63] ROTSKOFF, G. M. and VANDEN-EIJNDEN, E. (2022). Trainability and accuracy of artificial neural networks: an interacting particle system approach. *Comm. Pure Appl. Math.* **75** 1889–1935. MR4465905
- [64] SANTAMBROGIO, F. (2015). *Optimal transport for applied mathematicians. Progress in Nonlinear Differential Equations and their Applications* **87**. Birkhäuser/Springer, Cham Calculus of variations, PDEs, and modeling. <https://doi.org/10.1007/978-3-319-20828-2> MR3409718
- [65] SCHIEBINGER, G., SHU, J., TABAKA, M., CLEARY, B., SUBRAMANIAN, V., SOLOMON, A., GOULD, J., LIU, S., LIN, S., BERUBE, P. et al. (2019). Optimal-transport analysis of single-cell gene expression identifies developmental trajectories in reprogramming. *Cell* **176** 928–943.
- [66] SHAHAN, R., HSU, C.-W., NOLAN, T. M., COLE, B. J., TAYLOR, I. W., GREENSTREET, L., ZHANG, S., AFANASSIEV, A., VLOT, A. H. C., SCHIEBINGER, G. et al. (2022). A single-cell Arabidopsis root atlas reveals developmental trajectories in wild-type and cell identity mutants. *Developmental cell* **57** 543–560.
- [67] SHALEK, A. K., SATIJA, R., SHUGA, J., TROMBETTA, J. J., GENNERT, D., LU, D., CHEN, P., GERTNER, R. S., GAUBLomme, J. T., YOSEF, N. et al. (2014). Single-cell RNA-seq reveals dynamic paracrine control of cellular variation. *Nature* **510** 363–369.
- [68] SIRIGNANO, J. and SPILIOPOULOS, K. (2020). Mean field analysis of neural networks: A law of large numbers. *SIAM Journal on Applied Mathematics* **80** 725–752.
- [69] STREETS, A. M. and HUANG, Y. (2014). How deep is enough in single-cell RNA-seq? *Nature biotechnology* **32** 1005–1006.
- [70] TOWNES, F. W., HICKS, S. C., ARYEE, M. J. and IRIZARRY, R. A. (2019). Feature selection and dimension reduction for single-cell RNA-Seq based on a multinomial model. *Genome biology* **20** 1–16.
- [71] TRAAG, V. A., WALTMAN, L. and VAN ECK, N. J. (2019). From Louvain to Leiden: guaranteeing well-connected communities. *Scientific reports* **9** 1–12.
- [72] TRILLOS, N. G., KIM, J. and JACOBS, M. (2024). The multimarginal optimal transport formulation of adversarial multiclass classification. *J. Mach. Learn. Res.* **24**.
- [73] GARCÍA TRILLOS, N. and MURRAY, R. W. (2022). Adversarial Classification: Necessary Conditions and Geometric Flows. *Journal of Machine Learning Research* **23** 1–38.
- [74] VAN DIJK, D., SHARMA, R., NAINYS, J., YIM, K., KATHAIL, P., CARR, A. J., BURDZIAK, C., MOON, K. R., CHAFFER, C. L., PATTABIRAMAN, D. et al. (2018). Recovering gene interactions from single-cell data using data diffusion. *Cell* **174** 716–729.
- [75] VILLANI, C. (2003). *Topics in optimal transportation. Graduate Studies in Mathematics* **58**. American Mathematical Society, Providence, RI. <https://doi.org/10.1090/gsm/058> MR1964483
- [76] VILLANI, C. (2009). *Optimal transport. Grundlehren der mathematischen Wissenschaften [Fundamental Principles of Mathematical Sciences]* **338**. Springer-Verlag, Berlin Old and new. <https://doi.org/10.1007/978-3-540-71050-9> MR2459454
- [77] VIRSHUP, I., RYBAKOV, S., THEIS, F. J., ANGERER, P. and WOLF, F. A. (2021). anndata: Annotated data. *bioRxiv*. <https://doi.org/10.1101/2021.12.16.473007>

- [78] WANG, J., HUANG, M., TORRE, E., DUECK, H., SHAFFER, S., MURRAY, J., RAJ, A., LI, M. and ZHANG, N. R. (2018). Gene expression distribution deconvolution in single-cell RNA sequencing. *Proceedings of the National Academy of Sciences* **115** E6437–E6446.
- [79] WANG, G., JIAO, Y., XU, Q., WANG, Y. and YANG, C. (2021). Deep generative learning via Schrödinger bridge. In *International conference on machine learning* 10794–10804. PMLR.
- [80] WEISSMAN, T., ORDENTLICH, E., SEROUSSI, G., VERDU, S. and WEINBERGER, M. J. (2003). Inequalities for the L1 deviation of the empirical distribution.
- [81] WOLF, F. A., ANGERER, P. and THEIS, F. J. (2018). SCANPY: large-scale single-cell gene expression data analysis. *Genome biology* **19** 1–5.
- [82] ZHANG, M. J., NTRANOS, V. and TSE, D. (2020). Determining sequencing depth in a single-cell RNA-seq experiment. *Nature communications* **11** 774.